NASA Technical Paper 3017

September 1990

Modification of the SHABERTH Bearing Code To Incorporate RP–1 and a Discussion of the Traction Model

Claudia M. Woods

NASA

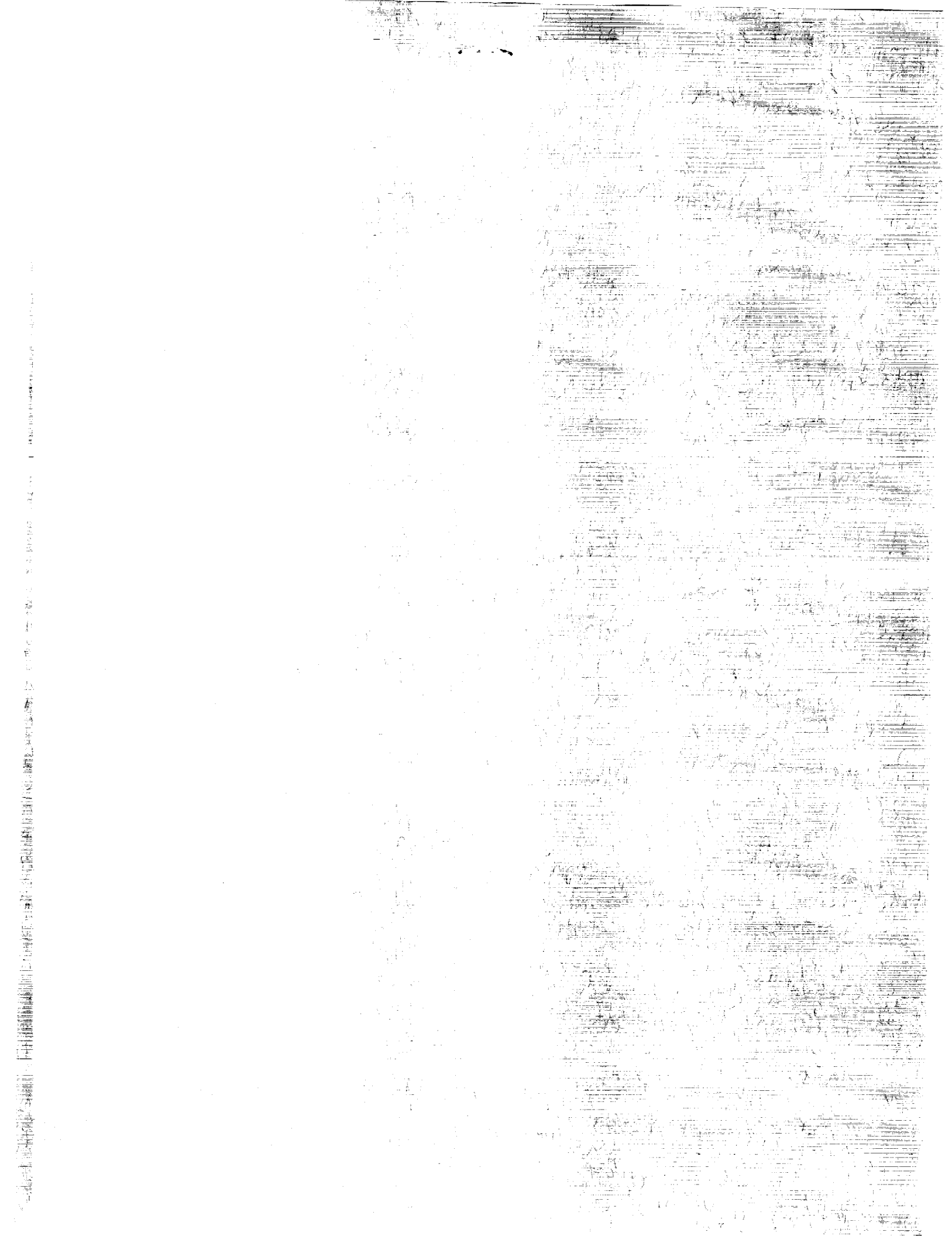

NASA Technical Paper 3017

1990

Modification of the SHABERTH Bearing Code To Incorporate RP–1 and a Discussion of the Traction Model

Claudia M. Woods
Lewis Research Center
Cleveland, Ohio

National Aeronautics and Space Administration
Office of Management
Scientific and Technical Information Division

Summary

Recently developed traction data for Rocket Propellant 1 (RP-1), a hydrocarbon fuel of the kerosene family, were used to develop the parameters needed by the bearing code SHABERTH in order to include RP-1 as a lubricant choice. As an aid to future additions, a review of the procedure for inputting data for a new lubricant choice is presented. In particular, the fluid traction model used by SHABERTH is discussed, and issues concerning it are presented. In the process of fitting the RP-1 traction data to the model, certain assumptions and simplifications were necessary. The error resulting from making these simplifications is discussed.

A slight error was detected in the traction equations that are in the SHABERTH program, but a lack of traction data on the original lubricants prevented immediate correction of the error. However, the error was judged insignificant to the traction prediction for RP-1. A temperature dependency that is not accounted for by the model was found in a particular traction coefficient for RP-1. The maximum traction coefficients that were predicted by using temperature-averaged coefficients erred by an average of 12 percent, whereas those predicted by using the discrete coefficients at the two temperature conditions erred by an average of 4 percent. Currently, the temperature-averaged coefficients are being used. The model of the pressure-viscosity coefficient as a function of temperature was modified for RP-1 by using pressure-viscosity data valid for RP-1.

Background

The introduction of reusable engines for space launch vehicles has made necessary the development of more rigorous design methodologies for long-life bearings in launch vehicle turbopump applications. Considerations of weight and simplicity require that the working fuel and oxidizer be used as the turbopump coolant and lubricant; however, there is currently a lack of data on the rheological properties of the types of fluids used in these applications at the conditions present in a bearing contact (i.e., high pressures and potentially high shear rates).

One fuel that has been considered for use in future launch vehicles (e.g., the advanced launch system (ALS)) is Rocket Propellant 1 (RP-1), a type of kerosene. Though RP-1 has been used in the past to cool and lubricate the bearings of expendable launch vehicles, such as Titan, only a small amount of data on its rheological properties has been collected (refs. 1 to 3).

In order to design long-life bearings to be run in RP-1, the bearing behavior needs to be theoretically analyzed. One of the most widely used rolling-element-bearing design and analysis tools is the computer code SHABERTH (Shaft Bearing Thermal Analysis, ref. 4). SHABERTH simulates the thermomechanical performance of a load support system consisting of up to five ball, cylindrical, or tapered-roller bearings. Transient or steady-state temperatures can be calculated by using a lumped-mass thermal model that takes into account free convection, forced convection, conduction, radiation, and mass transport heat transfer.

Since the SHABERTH code takes into account the influence of the lubricating fluid on bearing behavior, it requires certain empirical rheological data for the particular fluid. The SHABERTH code currently contains hard-coded rheological data on a number of lubricants. These data consist of density; thermal coefficient of expansion; thermal conductivity; the relationships of viscosity and temperature, and pressure-viscosity coefficient and temperature at ambient pressure; and the characteristics of fluid traction as a function of shear rate.

The rheological properties of RP-1, a low-viscosity fuel, differ greatly from those of the lubricating oils currently in the program as lubricant choices; therefore, the SHABERTH code had to be modified to include RP-1. The density, thermal expansion, and thermal conductivity, as well as data for viscosity with respect to temperature and for the pressure-viscosity coefficient as a function of temperature were available. The characteristics of traction force as a function of shear rate, however, needed to be established. Once all of the rheological data were established, they had to be fit to the various rheological models used by the code; this determined the inherent parameters that needed to be hard-coded into the SHABERTH code.

Introduction

The purposes of this report are (1) to review the general procedure for inputting data for a new lubricant choice into the SHABERTH bearing code and to describe the theoretical traction model used by SHABERTH, (2) to describe the fitting of the experimental RP-1 fluid traction data to the model, and

(3) to present results and quantify the error due to making certain assumptions. All RP-1 parameters needed by SHABERTH to run the program are specified.

As previously mentioned, in order to predict the behavior of a bearing being lubricated and cooled by a specific fluid, the SHABERTH bearing code requires empirically derived rheological data on the fluid (viscosity-temperature relationship, density, thermal expansion, thermal conductivity, pressure-viscosity coefficient, and traction force as a function of shear rate). The experimental data must be fit to various rheological models that the code uses to determine the values of specific parameters for that fluid. These values must then be hard-coded. A review of the entire procedure is presented to aid in future lubricant additions. This review utilizes material from references 4 to 6. In particular, the fluid traction model used by the SHABERTH code is discussed in detail.

Experimental viscosity-temperature, density, thermal expansion, and thermal conductivity data for RP-1 were obtained from reference 7. The experimental characteristics of traction force as a function of shear rate needed to be established. The traction force in a bearing contact is dependent not only on shear rate (or sliding velocity) but also on the maximum Hertzian contact pressure, the rolling velocity, and the temperature of the fluid in the contact. An effort was made to obtain experimental data on the traction coefficient as a function of sliding velocity for RP-1 fuel at various conditions of maximum contact pressure, rolling velocity, and temperature. The work was conducted on a twin disk traction tester by using side slip to produce the traction. Further information on the testing can be found in reference 8, where RP-1 data pertaining to the pressure-viscosity coefficient at ambient pressure as a function of temperature, which was used to modify the SHABERTH code, can also be found.

Fitting the experimental data to the rheological models is straightforward for all but the fluid traction model. Therefore, only the fitting of the RP-1 fluid traction data to the fluid traction model will be discussed in detail. The necessary parameters for all of the models will be specified.

In the process of fitting the RP-1 traction data to the traction model that exists in the code, certain assumptions and simplifications were necessary. The error due to making these simplifications is quantified by comparing theoretical predictions of traction force with and without the simplifications to each other and to the experimental data.

Review and Discussion of the SHABERTH Rheological Models

Fluid Property Models

This section describes the density, thermal conductivity, viscosity and temperature, and pressure-viscosity and temperature models already in the SHABERTH code (see ref. 6). Values for the parameters within the models for RP-1 are listed in appendix A.

Although the SHABERTH code requires the user input file to be in SI units and furnishes the output in SI units, the internal calculations are all done in English units. Also, some of the models used are based on empirical equations that were developed by using a mixture of SI and English units. Therefore, some variation occurs in the system of units required for each piece of property data that must be hard-coded. The proper units for each piece of information are specified. All symbols are defined in appendix B.

Density, thermal expansion coefficient, and thermal conductivity.—The SHABERTH code assumes a linear relationship between fluid density and temperature, with the thermal expansion coefficient being the slope. The necessary parameters are the fluid density ρ (in g/cm^3 at 60 °F) and the thermal expansion coefficient G (in (g/cm^3)/°C), which can be obtained as the slope of the line of the specific gravity plotted as a function of temperature T. The code internally converts G to degrees Fahrenheit and calculates density using

$$\rho[T] = \rho \text{ (at } 60 \text{ °F)} - G \text{ (at } T - 60 \text{ °F)} \tag{1}$$

The thermal conductivity of the fluid K_f', which must be expressed in the code in watts/meter °C, is assumed to be constant with temperature. In actuality, it varies slightly with temperature, so the user must choose the specific temperature at which to take the thermal conductivity data.

Viscosity as a function of temperature.—The kinematic viscosity ν in centistokes (cSt) at atmospheric pressure is calculated as a function of temperature from Walther's relation (ref. 6)

$$\log_{10}[\log_{10}(\nu + 0.6)] = A - B \log_{10}(T + 459.7) \tag{2}$$

A and B are lubricant-dependent constants determined by substituting into equation (2) the experimental data of kinematic viscosity ν (in cSt) as a function of temperature T (in °F).

SHABERTH calculates the absolute viscosity at ambient pressure η_0' in centipoise (cP) using

$$\eta_0' = \nu\rho \tag{3}$$

The necessary parameters for the code are A, B, and ν at both 100 and 210 °F, in cSt.

An auxiliary temperature-viscosity coefficient β (in 1/°R), which is needed for use in a film-thickness thermal reduction factor, is found by calculating

$$\beta = 0.00909 \ln\left(\frac{\eta_0 \text{ (at } 100 \text{ °F)}}{\eta_0 \text{ (at } 210 \text{ °F)}}\right) \tag{4}$$

Pressure-viscosity coefficient as a function of temperature.—The SHABERTH code calculates the value of the pressure-viscosity coefficient α (in^2/lb) at atmospheric pressure and a given temperature by using the following relationship developed by Fresco (ref. 6):

$$\alpha = (2.303 \times 10^{-4}) \left| C_F + D_F \log_{10}(\nu) + E_F \left\{\log_{10}(\nu)\right\}^2 \right|^{TF} \tag{5}$$

where

TF	$560/(T + 459.7)$
ν	$\nu_1 T$
C_F, D_F, E_F	constants determined by Fresco
T	temperature, °F

The values of C_F, D_F, and E_F are constant for all lubricant types, so no further data are needed for the particular fluid. However, whether this model will adequately predict pressure-viscosity coefficients for fluids that differ greatly from the original lubricating oils in the code is questionable. This will be discussed in the section Pressure–Viscosity Coefficient for RP-1.

Traction

In this section, the traction curve is defined and the SHABERTH traction model is described. All symbols are defined in appendix B.

The traction curve.—Tevaarwerk (ref. 9) defines traction as "the ability of a fluid film, trapped under high pressure in the elastically deformed region of two loaded curved elements, to transmit a tangential force from one element to the other." The characteristics of traction variation with shear rate for a fluid have an important effect on the behavior of the contacting bodies separated by the fluid, both in the motion of the bodies and in the amount of heat generated between them. When two contacting rolling elements that are separated by a fluid have different surface speeds, tangential forces develop at the area of contact. These forces, which arise from the shearing of the fluid layer, are a function of the rate of shear of the fluid. They are also a function of the type of fluid and of the maximum Hertzian contact pressure, rolling velocity, and fluid temperature within the contact area. Therefore, the traction characteristics of a fluid must be determined experimentally for each fluid. This can be done by rotating two disks against one another and introducing a measurable amount of slip between them while using the fluid in question as the lubricant. Curves of traction force as a function of sliding rate can be obtained at various conditions of maximum contact pressure P_o, rolling velocity V, and fluid temperature T. Figure 1 shows a rolling-element contact shearing a fluid film of thickness h. The variable P is the idealized Hertzian pressure distribution across the contact. Shear stresses τ_x, which develop because of the difference in surface speeds, affect the heat generation and the tangential forces acting on the rolling elements.

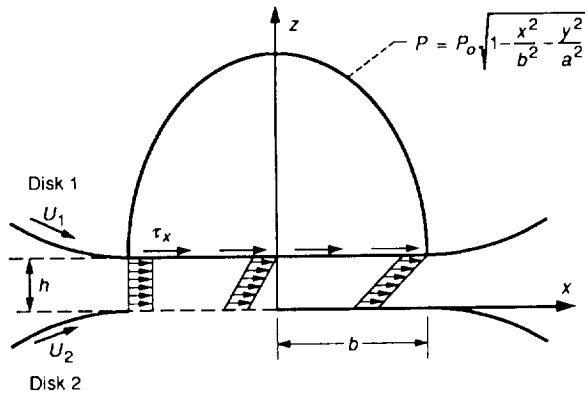

Figure 1.—Rolling-element contact showing film of oil under shear; $u_s = U_1 - U_2 \neq 0$.

In an actual contact, the shear stress and the shear rate vary across the thickness of the film. It is common practice, however, to treat the problem as if the shear takes place at one plane of the film, with the fluid entrained by disk 1 traveling at surface speed U_1 and the fluid entrained by disk 2 traveling at surface speed U_2. Therefore, the relationship of shear stress to shear rate can be characterized by measuring the total traction force as a function of measurable values of sliding speed u_s, or slip, where

$$u_s = U_1 - U_2 \tag{6}$$

The entrainment, or rolling, velocity V of the fluid is taken to be

$$V = \frac{U_1 + U_2}{2} \tag{7}$$

Figure 2 shows the typical shape of the curve for traction as a function of sliding speed. Traction force is expressed in terms of a traction coefficient μ where

$$\mu = \frac{\text{traction force}}{\text{normal load}} \tag{8}$$

Three distinct regions can be identified on this curve. The initial low-slip region of the curve is linear and is thought to be isothermal in nature. At some sliding speed the traction behavior becomes nonlinear, though still increasing. This region is also thought to be isothermal. In the third region, the heat generated by dissipative shearing of the fluid is no longer negligible. This region is characterized by either decreasing traction with further increases in sliding velocity or a flattening of the curve towards a horizontal asymptotic line.

The magnitude of a traction curve at particular conditions can be characterized by the maximum traction coefficient reached on the curve. Again, this is a function of maximum

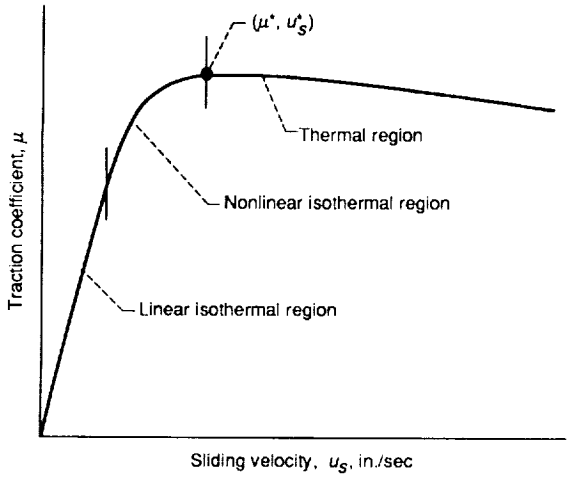

Figure 2.—Traction coefficient μ as a function of sliding velocity u_s.

contact pressure, rolling velocity, and fluid temperature. The maximum traction coefficient is denoted by μ^*, and the sliding velocity at which μ^* occurs is denoted by u_s^*.

The SHABERTH traction model.—This discussion applies to the SHABERTH/SKF traction model, not the SHABERTH/NASA model. The differences between the two are discussed in reference 4. The complete SHABERTH/SKF traction model comprises an asperity traction model and a fluid-film traction model. The lubricant traction characteristics are required only for the fluid traction model. SHABERTH calculates h/σ, that is, the ratio of film thickness h to composite surface roughness σ. For $h/\sigma < 0.4$, traction is modeled as purely asperity contact. For $h/\sigma > 3.0$, the traction model is purely lubricant-dependent. For $0.4 < h/a < 3.0$, the model is a combination of the asperity and fluid-film models (ref 6).

The development of the SHABERTH fluid traction model is explained in reference 5. Since English-system units are used in the reference material, they are used here to describe the model and to fit data to it. Basically, the energy and momentum equations were developed in order to find the governing dimensionless terms. Such terms for heat conduction and convection, slide-to-roll ratio, and the speed-viscosity product ($U = \eta_0 V\alpha/R_x$) are included in these equations. The total thermal effect was assumed to be a multiplicative power function of the individual thermal dimensionless terms, for which the exponents were unknown. Adding a viscoelastic correction to the effective viscosity term produced a relationship between a nondimensional traction coefficient term μ' and a nondimensional sliding-speed term $\psi_0^{1/2}$. (Further explanation of the nondimensionalization process can be found in ref. 5.) The exponents of the thermal terms were determined by using Johnson and Cameron's experimental data for a mineral oil, Shell Turbo 33 (ref. 10). The ensuing curve of μ' as a function of $\psi_0^{1/2}$ is constant over all maximum contact pressures, rolling velocities, and temperatures, for all choices of lubricants; it is the curve to which data for all other lubricant choices for the program are fit. The maximum nondimensional traction coefficient term on the curve is designated by $(\mu')^*$, and $(\psi_0^{1/2})^*$ is the nondimensional sliding-speed term at which $(\mu')^*$ occurs. These values which were obtained by using the Johnson-Cameron data, are constant:

$$(\mu')^* = 0.235 \quad \text{and} \quad (\psi_0^{1/2})^* = 8.75\times10^{-5} \tag{9}$$

From these values an equation is obtained for the maximum traction coefficient μ^* at particular conditions, and for the associated sliding speed u_s^* as a function of those conditions (ref. 5), as follows:

$$0.235 = \mu^* \frac{P_e h\beta^{1/2}}{(K_f\eta_e)^{1/2}} \left(\frac{bK_f}{\rho_f C_f V h^2}\right)^{0.28} \left(\frac{K_f}{\eta_e\beta V^2}\right)^{0.11} \left(\frac{\eta_0 V\alpha}{R_x}\right)^{0.02} \tag{10}$$

and

$$8.75\times10^{-5} = \left(\frac{u_s^*}{V}\right) \left(\frac{bK_f}{\rho_f C_f V h^2}\right)^{0.28} \left(\frac{\eta_e\beta V^2}{K_f}\right)^{0.4} \left(\frac{\eta_0 V\alpha}{R_x}\right)^{0.7} \tag{11}$$

Four other lubricants have been added to the SHABERTH code. They are a polyphenyl ether (5P4E), MIL-L-7808 oil, MIL-L-23699 oil, and a fluorinated polyether (Freon E-1).

Calculation of the Fluid Traction Parameters for SHABERTH

In this section, the procedure for finding the fluid traction parameters is described. Thereafter, a discussion of concerns with the model and with the potential difficulties that can be encountered in fitting the data is presented.

There are three basic steps involved in fitting fluid traction data to the SHABERTH fluid traction model: (1) traction data obtained for an elliptical contact must first be transformed into equivalent traction data that would occur over a rectangular contact at the same conditions; (2) the parameters that govern the values of μ^* and u_s^* must be determined from the transformed values of the experimental data; and (3) parameters governing the shape of the curve of μ as a function of u_s are determined from the transformed data.

Transformation from elliptical- to line-contact data.—The SHABERTH traction model was developed on the basis of a rectangular, or "line," contact (ref. 5). When analyzing an elliptical contact, the SHABERTH code divides the contact into discrete rectangular strips, the length of the strips being in the rolling (x) direction as in figure 3. SHABERTH then calculates a traction force for each strip and integrates the traction force over the elliptical contact. Experimental traction data obtained over an elliptical contact must be transformed to the equivalent traction data that would occur over a line contact at the same contact conditions. McCool et al. (ref. 5) developed a method for this transformation.

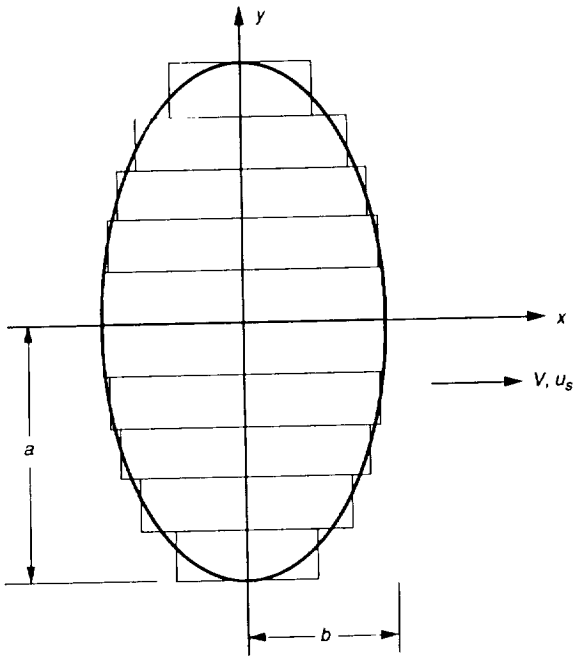

Figure 3.—Rolling-element contact ellipse showing discrete rectangular strips utilized by SHABERTH.

The pressure distribution over a line contact is assumed to be constant in the rolling direction and to vary semielliptically (as shown in fig. 1) along the semimajor (y) axis; that is, strip to strip. If the pressure distribution and geometry of the equivalent line contact, and the traction force-pressure relationship are known, the traction force over the contact can be calculated. The traction force-pressure relationship, which varies with rolling velocity, temperature, and sliding velocity, can be found from the experimental elliptical traction data.

The measured total traction force T_R is divided by the length $2a$ of the elliptical contact in the y-direction to obtain an average traction force per unit length $\bar{T}_R$. Then a relationship must be found between T_R and P_o; this is possible with the assumption that a polynomial relationship can reasonably model the data for $\bar{T}_R$ as a function of P_o, while remaining easy to integrate analytically. Therefore, a general relationship of the form

$$T_R = d_0 + d_1 P_o + d_2 P_o^2 + d_3 P_o^3 + d_4 P_o^4 \tag{12}$$

where

$d_0, d_1, d_2, \ldots$	polynomial coefficients to be determined
$\bar{T}_R$	$T_R/2a$
T_R	measured traction force
a	contact semimajor length

was integrated over the line contact to obtain an expression for equivalent average traction per unit length, over a line contact, as a function of P_o. From this integrated expression and the original polynomial of equation (12), the following relationship between the elliptical-and the line-contact traction coefficients was obtained (it requires only the polynomial coefficients $d_0, d_1, \ldots$, and the maximum Hertzian pressure of the particular elliptical contact):

$$\frac{\mu_{\text{line}}}{\mu_{\text{elliptical}}} = \left(\frac{4}{3\pi}\right) \frac{G_0 + G_1 P_o + G_2 P_o^2 + G_3 P_o^3 + G_4 P_o^4}{d_0 + d_1 P_o + d_2 P_o^2 + d_3 P_o^3 + d_4 P_o^4} \tag{13}$$

where

G_0 $(\pi/2)d_0$

G_1 $2d_1$

G_2 $(3\pi/4)d_2$

G_3 $(8/3)d_3$

G_4 $(15\pi/16)d_4$

For a particular fluid, at each condition of rolling velocity, temperature, and sliding velocity, the experimental data for average traction force T_R as a function of maximum contact pressure P_o are fit to equation (12) in order to find the polynomial coefficients. These coefficients and the particular contact pressure of interest are substituted into equation (13), whereby equivalent traction coefficient data over a line contact are determined.

Traction parameters governing the maximum traction coefficient and the sliding velocity of maximum traction.— The traction parameters needed by SHABERTH to find the values of μ^* and u_s^* at particular contact conditions are those dealing with the viscoelastic relationship and some proportionality constants.

The viscoelastic relationship defines an effective fluid viscosity η_e, at contact conditions, as a function of ambient fluid viscosity η_0, contact pressure P_o, and fluid entrainment velocity V. The viscoelastic model in SHABERTH is of the form

$$\eta_e = \eta_0 f(P_o) \left(\frac{V}{V_0}\right)^{-\lambda_0} \tag{14}$$

where $f(P_o)$ and $(V/V_0)^{-\lambda_0}$ are viscoelastic corrections for the pressure and the entrainment velocity, respectively. The viscoelastic parameters that must be found for each new lubricant are $f(P_o)$ and λ_0.

The exponent λ_0 is obtained by fitting the experimental data for μ^* as a function of V, at constant temperature and pressure, to a relationship of the form

$$\mu^* = C_m V^{\gamma_3} \tag{15}$$

where C_m is a constant of proportionality and by defining γ_3 as

$$\gamma_3 = a_3 + 0.5\lambda_0(a_1 + a_2) - \lambda_0 - c_1 + n_1(a_2 - 1) + 0.5a_2 \tag{16}$$

where

$a_1 = 0.236$

$a_2 = 0.55$

$a_3 = 0.22$

$c_1 = 0.022$

The coefficients a_1,a_2,a_3,c_1 were developed from the Johnson-Cameron data. The term n_1 is the exponent of the rolling speed from the film thickness relationship. With a value of $n_1 = 0.7$ taken for a typical unstarved contact, the equation reduces to

$$\lambda_0 = \frac{0.165 - \gamma_3}{0.607} \tag{17}$$

The function $f(P_o)$ is found by using equation (10) and the experimental contact conditions and traction data to calculate values of η_e as a function of P_o. From the viscoelastic relationship,

$$f(P_o) = \left(\frac{\eta_e}{\eta_0}\right)\left(\frac{V}{V_0}\right)^{\lambda_0} \tag{14}$$

$f(P_o)$ can be found as a function of P_o since λ_0 has been calculated previously. The constant V_0 will be discussed shortly.

The SHABERTH model for $f(P_o)$ was developed from the Johnson-Cameron data. Figure 4 shows the relationship obtained from these data plotted on log-log coordinates. This figure shows not only that the relationship is exponential but also that the value of the exponent changes at a certain pressure. Therefore, the relationship is modeled as a function of the form

$$f(P_o) = C_n\left(\frac{P_o}{P_1}\right)^{A_i} \tag{18}$$

where

$A_i = A_1$, for $P_o < P_1$

$A_i = A_2$, for $P_o \geq P_1$

and A_1, P_1, and C_n are lubricant-dependent constants.

The value of P_1 is chosen as the pressure (in lb/in$^2 \times 10^{-5}$) at which the slope of the log-log plot of $f(P_o)$ as a function of P_o changes. The value of A_1 is chosen from the best-fit value of the exponent A_i over all conditions prior to P_1, and A_2 is the best-fit exponent at pressures greater than or equal to P_1. The value of C_n need not be determined from this data fit because it is combined with other constants to form general proportionality constants C_1 and C_2, which are determined after all of the specific parameters are found.

By substituting the viscoelastic relationship into equations (10) and (11) and by grouping the fluid property constants into general proportionality constants, the following equations,

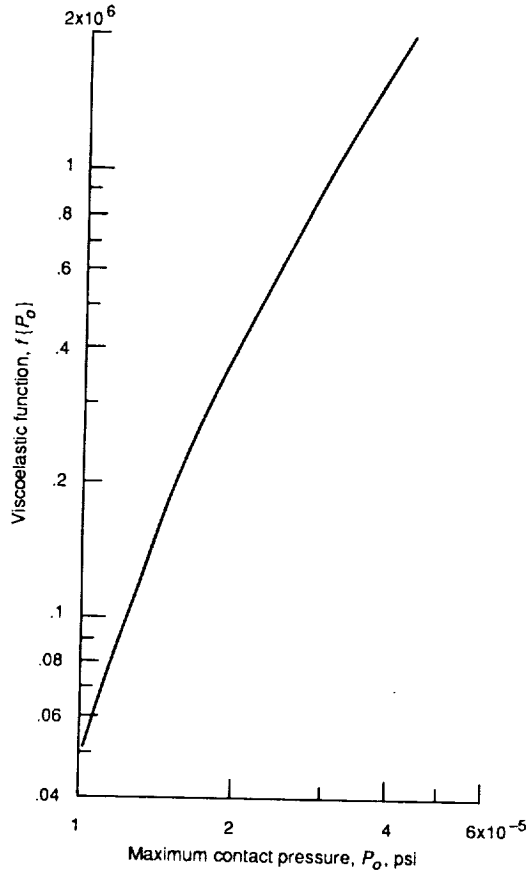

Figure 4.—Variation of viscoelastic function $f(P_o)$ with maximum contact pressure for Shell Turbo 33 oil used to develop SHABERTH fluid traction model.

relating μ^* and u_s^* to P_o, V, η_0, and h, are obtained:

$$\mu^* = (C_1)P_o^{-1.14}\left(\frac{P_o}{P_1}\right)^{0.61A_i}\eta_0^{0.59}V^{(0.48-0.61\lambda_0)}h^{-0.45} \tag{19}$$

and

$$u_s^* = (C_2)P_o^{-0.14}\left(\frac{P_o}{P_1}\right)^{-0.4A_i}\eta_0^{-1.1}V^{(0.4\lambda_0-0.09)}h^{-0.55} \tag{20}$$

where

$A_i = A_1$, for $P_o < P_1$

$A_i = A_2$, for $P_o \geq P_1$

By substituting experimental values of μ^* and u_s^*, at the specific test conditions, into equations (19) and (20), best-fit values of C_1 and C_2 can be determined. These equations are used in the SHABERTH code, along with lubricant-specific values of λ_0, P_1, A_1, A_2, C_1, and C_2, to predict values of μ^* and u_s^*.

The constant V_0, which serves as a rolling velocity normalization factor, is not a required parameter in the SHABERTH code. It is used only when a relationship between $f(P_o)$ and

P_o is fitted by using equation (14). For each of the oils discussed in reference 5, the value chosen for V_0 was that of the lowest rolling velocity condition in the particular test matrix. However, for the model of $f(P_o)$ shown in equation (18) (an exponential relationship), the value of V_0 has no effect on the relevant parameters that are being determined (i.e., the values of A_1, A_2, and P_1); its only effect is to shift the curve of $\log[f(P_o)]$ as a function of $\log[P_o]$ by a constant factor. The values of the proportionality constants C_1 and C_2 are determined from equations (19) and (20), which do not include the constant V_0.

Modeling the shape of the traction curve.—Once the theoretical value of μ^* has been determined by SHABERTH for certain contact conditions, the shape of the curve of the traction coefficient as a function of sliding velocity is needed to determine μ at a particular sliding velocity. Experimentally derived traction curves are of two basic types (see fig. 5). For both types, μ increases linearly at low sliding speeds and then becomes nonlinear, increasing at a slower rate. The curve shown in figure 5(a) reaches the value of μ^* and then slowly decreases with increasing sliding speed. The curve shown in figure 5(b) increases continuously to an asymptotic value of μ^*. SHABERTH uses the continuously increasing, asymptotic model; the other model created convergence problems in the program.

Values must be found for the coordinates where the linearly increasing portion of the asymptotic curve ends. These values are dependent on the contact conditions. However, the experimental data for all contact conditions falls on a single curve of (μ/μ^*) as a function of (u_s/u_s^*). Therefore, SHABERTH models the shape of the traction curve on the basis of one set of coordinates, (X_B, Y_B), where the linear portion of the experimental curve of (μ/μ^*) as a function of (u_s/u_s^*) ends (see fig. 6). The SHABERTH code then calculates values of μ using

$$\frac{\mu}{\mu^*} = \left(\frac{Y_B}{X_B}\right)\left(\frac{u_s}{u_s^*}\right) \qquad 0 \le \frac{u_s}{u_s^*} \le X_B$$

and

$$\frac{\mu}{\mu^*} = Y_B\left(1 + \frac{Y_D X_D}{Y_D X_B + Y_B X_D}\right) \qquad \frac{u_s}{u_s^*} > X_B \qquad (21)$$

where

$Y_D \quad 1 - Y_B$

$X_D \quad (u_s/u_s^*) - X_B$

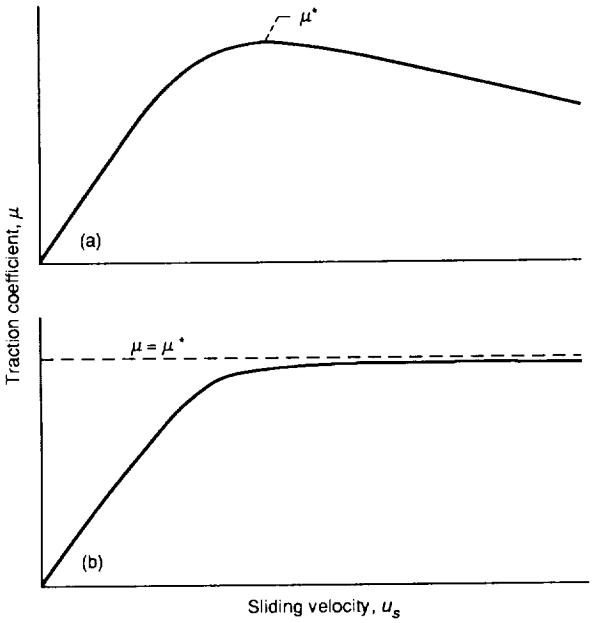

(a) Curve exhibiting peak behavior.
(b) Asymptotic behavior model used in SHABERTH code.

Figure 5.—Two types of behavior exhibited by curves of experimental traction coefficient as a function of sliding velocity.

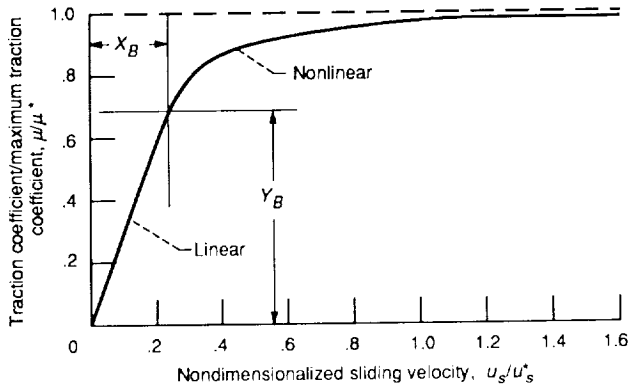

Figure 6.—Nondimensionalized traction curve showing coordinates (X_B, Y_B) used to define shape of curve.

Issues Concerning the SHABERTH Fluid Traction Model

Issues relevant to the SHABERTH fluid traction model and the problems that can arise during the fitting of the experimental traction data and the extraction of the parameters are discussed.

Transformation from elliptical- to line-contact data.—Care must be taken when fitting a polynomial to the elliptical-contact data of T_R as a function of P_o. As previously discussed, the resulting polynomial models the relationship between T_R and P as it varies over a rectangular (line) contact. Equation (13) was developed by integrating a general form of the polynomial across incremental strips of a line-contact area for which the pressure is P_o at the center strip and decreases semielliptically toward the edge of the contact in the y-direction. Therefore the polynomial for each set of contact conditions must be valid down to pressures below P_o.

Figure 7 shows a possible example of a polynomial fit to experimental data. The points A, B, C, and D represent

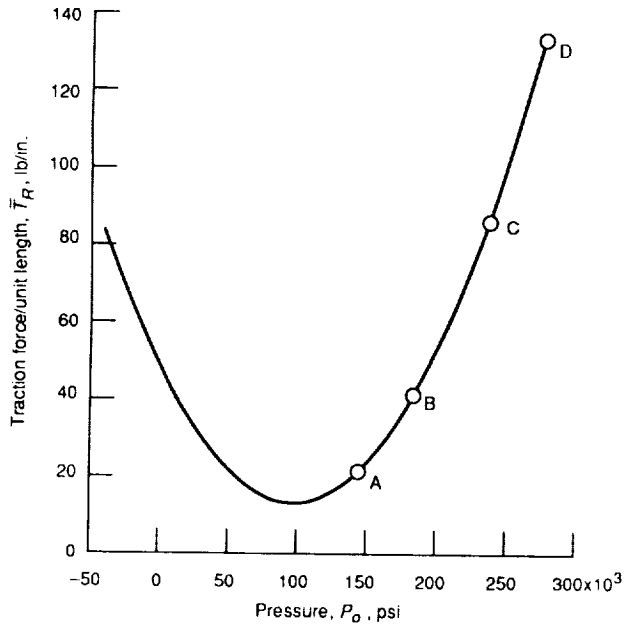

Figure 7.—Example of a polynomial fit through four points representing experimental data.

experimental data points. As P decreases, the polynomial reaches a minimum and then begins increasing at values of P not far below the value of P_o for conditions at point A—behavior which is not valid for traction as a function of pressure.

If the polynomial coefficients obtained from the original four data points are used in equation (13) for the maximum pressure condition at point A, and to a lesser degree at conditions of point B, the resulting $\mu_{line}/\mu_{elliptical}$ values are often implausible. This problem was first encountered with the RP-1 experimental traction data. Since there were only four conditions of pressure for the fit, second-order polynomials were used. Reference 5 contains experimental elliptical-contact data and equivalent transformed line-contact data for a polyphenyl ether (5P4E), which had a test matrix containing three conditions of pressure. When the transformation method was applied to this elliptical data, also using second-order polynomials, the same problems occurred as with the RP-1 data. The transformed line-contact data for 5P4E, obtained at the lowest two conditions of P_o by using polynomials fit to the listed experimental traction data, often did not match the original transformed data listed in reference 5. Also, they were not reasonably expected values. When the polynomials for these cases were examined, they exhibited behavior such as shown in figure 7. The erroneous increase of $\bar{T}_R$ at pressures still well within the contact ellipse has a profound effect on the resulting $\mu_{line}/\mu_{elliptical}$ values.

A method was found to solve this problem. First, fit a geometric relationship to the data of $\bar{T}_R$ as a function of P_o such that

$$T_R = b_1\left(b_2^{P_o}\right) \tag{22}$$

where b_1 and b_2 are coefficients of the geometric fit.

An advantage of this relationship is that T_R goes to zero as P_o goes to zero, which is in keeping with physical reality. By using equation (22), values of T_R at pressures below the lowest test matrix P_o were predicted. Then the original and predicted data for T_R as a function of P_o were used together to fit a polynomial of the form of equation (12). The resulting set of polynomial coefficients (d_0, etc.) were used in equation (13) to obtain final values of $\mu_{line}/\mu_{elliptical}$. For 5P4E the results of this method were in good agreement with the original transformed line-contact data listed in reference 5 for all conditions. Another method was also tried, using an exponential relationship of the form $T_R = b_3(P_o^{b_4})$ in place of equation (22), but these results did not agree as well with the original 5P4E data. Therefore, the method that uses equation (22) is recommended.

Viscoelastic parameters.—The model of $f(P_o)$ as a function of P_o shown in equation (18) was developed from experimental data that exhibited a change in the value of A_i at a pressure P_1 within the experimental test matrix; it is embedded in the final traction equations used in the SHABERTH code. Therefore, values for A_1, A_2, and P_1 must be obtained for each new lubricant.

However, it is not clear what procedure should be used to determine values for P_1 and A_2 when they do not occur within the pressure range over which the experimental data were taken. The $f(P_o)$ data shown in reference 5 for the 5P4E and the MIL-L-7808 oils indicate that in neither case is there a change in the value of A_i at any place in the experimental pressure range. However, values of P_1 and A_2 were selected.

On the basis of the behavior of other fluids under high pressure (refs. 10 and 11), it is reasonable to assume that there is a pressure P_1 at which the value of the exponent A_i decreases from A_1 to some A_2. The data in reference 11 show that the pressure-viscosity coefficient α, normally associated with the simple power law $\eta = \eta_0 e^{\alpha P_o}$, decreases to $\beta' << \alpha$ at some pressure. The pressure-viscosity model of equation (18) is somewhat different than this one, but since equation (18) is still a power law, it would also be expected to exhibit a decrease in the value of the exponent A_i at some pressure.

It is impossible to know the exact value of P_1 without experimental data. A value should be chosen that gives some weight to the experimentally derived value of A_1; that is, a value which extends, somewhat, the range at which A_1 is valid beyond the highest pressure in the test matrix. However, the value chosen for P_1 should not be too much higher than the experimental range, since the error due to using A_1 at pressures where the actual behavior follows A_2 has exponential effects on the predicted values of viscosity. For the 5P4E and the MIL-L-7808 oils respectively, values of

P_1 were chosen that were 14 and 20 percent greater than the highest experimental contact pressure. This seems reasonable.

The only data available on which to base a choice of the value of A_2 are those of Johnson and Cameron for Shell Turbo 33. The most reasonable recourse seems to be to choose a value of A_2/A_1 based on A_2/A_1 for Shell Turbo 33 and then find A_2 from the value of A_1 for the particular fluid. For Shell Turbo 33, $A_2/A_1 = 0.635$.

In choosing a value of A_2/A_1 for other fluids, a more conservative prediction of viscosity is obtained by erring on the low side of the actual A_2 than by erring by the same amount on the high side, because of the exponential effect. Therefore, a value of less than 0.635 is recommended for A_2/A_1.

For the other original lubricants in the SHABERTH code, the following A_2/A_1 values were used: 5P4E, 0.456; MIL-L-7808, 0.363; and MIL-L-23699, 0.5.

Final fluid traction equations.—Equations (19) and (20) show the final equations used by the SHABERTH code to predict μ^* and u_s^* as functions of P_o, η_0, V, and h. However, a slight error has been detected in these formulas. In the original traction equations developed by McCool, et al. (ref. 5)

$$\mu^* = C_m P_o^{-1} b^{-0.28} h^{-0.45} \tag{23}$$

where

C_m proportionality constant

b $2\pi R_x(P_o)/E'$

h $C_q(\alpha\eta_0 V)^{0.7} P_o^{-0.3}$ for typical unstarved contact

Substituting the expression for b into equation (23) gives the relation

$$\mu^* = C_m P_o^{1.28} h^{-0.45} \tag{24}$$

The -1.28 value of the P_o exponent is that value for which h is still a separate variable in the equation. To find the total relationship between μ^* and P_o, the film thickness term h was broken up to give

$$\mu^* = C_m P_o^{-1.14} \tag{25}$$

Here, the -1.14 value of the P_o exponent is that for which h is no longer a variable in the equation.

In equations (19) and (20), however, h has been reintroduced as a variable. The exponents associated with η_0 and V are the appropriate ones since the film thickness term includes contributions of η_0 and V. The exponent of P_o, on the other hand, has been left as -1.14.

The corrected equations should read

$$\mu^* = (C_1) P_o^{-1.28} \left(\frac{P_o}{P_1}\right)^{0.61 A_i} \eta_0^{0.59} V^{(0.48 - 0.61\lambda_0)} h^{-0.45} \tag{26}$$

and

$$u_s^* = (C_2) P_o^{-0.28} \left(\frac{P_o}{P_1}\right)^{-0.44 A_i} \eta_0^{-1.1} V^{(0.4 - 0.09)} h^{-0.55} \tag{27}$$

where

$A_i = A_1$, for $P_o < P_1$

$A_i = A_2$, for $P_o \geq P_1$

The exponent of P_o cannot be easily changed in the program for the following reason: once A_1, A_2, λ_0, and P_1 have been determined from equations (17) and (18), the traction data are used to determine the values of C_1 and C_2 for each lubricant. The hard-coded values of C_1 and C_2 for the existing choices were calculated by using $P_o^{-1.14}$. Without the original traction data for these lubricants, the values of C_1 and C_2 associated with $P_o^{-1.28}$ cannot be calculated. The difference in traction prediction between the two sets of equations for the RP-1 data at the experimental conditions will be shown to be negligible.

Development of the SHABERTH Fluid Traction Parameters for RP-1

In this section, the experimental traction data for RP-1, a modified model of the pressure-viscosity coefficient for RP-1, and the fitting of the data to the SHABERTH fluid traction model are discussed.

Experimental Traction Data for RP-1

After a description of the RP-1 traction test matrix, the effect of transforming the experimental elliptical-contact traction data to equivalent line-contact traction data is shown. General trends of the transformed RP-1 data are also presented.

Test matrix conditions.—A twin disk tester generated data for traction force as a function of sliding speed for RP-1 fuel. An elliptical contact under various conditions of Hertzian pressure, rolling speed, and temperature (ref. 8) was used. The transverse radius of curvature of the lower disk was infinity; the upper disk was a toroid, the curvature of which produced the desired contact geometry. The traction data were generated with side slip, which can be produced by skewing the toroid about the normal to the horizontal plane. The slide-to-roll ratio u_s/V can be controlled and measured via the skew angle. The test matrix is listed in table I. Figure 8 shows a typical set of curves for experimental traction coefficient μ as a function of u_s/V for elliptical contact. This particular set of curves shows the variation of traction with rolling velocity at one condition of pressure and temperature. In general, traction decreases with increasing rolling velocity, increases with increasing pressure, and decreases with increasing temperature.

TABLE I.—TARGET TEST MATRIX CONDITIONS[a]

Hertzian pressure, GPa (kpsi)	1.01 (147)
	1.27 (185)
	1.60 (233)
	1.92 (279)
Rolling velocity, m/sec (in./sec)	10 (390)
	30 (1200)
	50 (2000)
Temperature, °C (°F)	40 (104)
	65 (149)

[a]All parameters were tested.

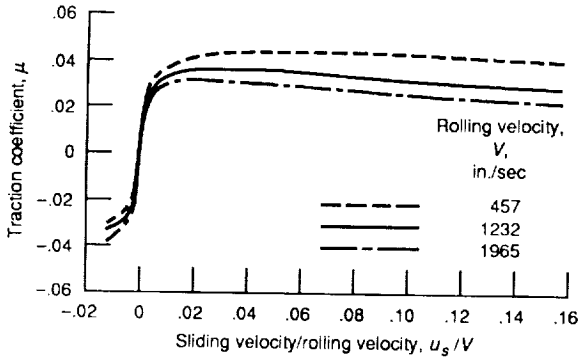

Figure 8.—Experimental traction coefficient as a function of slide-to-roll ratio for RP-1 at varying values of rolling velocity. Contact pressure, 279 kpsi; temperature, 111 °F.

The conditions shown in table I represent the maximum capabilities of the test rig. The upper limits extend above those of the original lubricants. For example, the Johnson-Cameron data had the highest Hertzian pressure condition at 225 000 psi (V_{max} = 1000 in./sec), and the MIL-L-7808 data included the highest rolling speed at 1820 in./sec ($P_{o\,max}$ = 150 000 psi). Values of Hertzian stress greater than the maximum in the RP-1 matrix would result in h/σ values that would trigger the asperity-contact-only traction model. Therefore, the test matrix shown in table I is quite adequate for the purpose of modeling the traction behavior of RP-1.

Transformation from elliptical-to line-contact data.—The RP-1 data were transformed from elliptical-to line-contact data by the method previously described. Since there were only four conditions of pressure in the fit, second-order polynomials were used. Figure 9 shows a comparison of the RP-1 curve of μ as a function of u_s/V for elliptical contact to that for the equivalent transformed line contact for RP-1 at one set of conditions. The elliptical-and line-contact curves at other conditions compare similarly. The equivalent line-contact data always exceed the elliptical-contact data, the greatest amount of difference being in the nonlinear region of low u_s/V. The line-to-elliptical ratio then decreases at increasing u_s/V. Also,

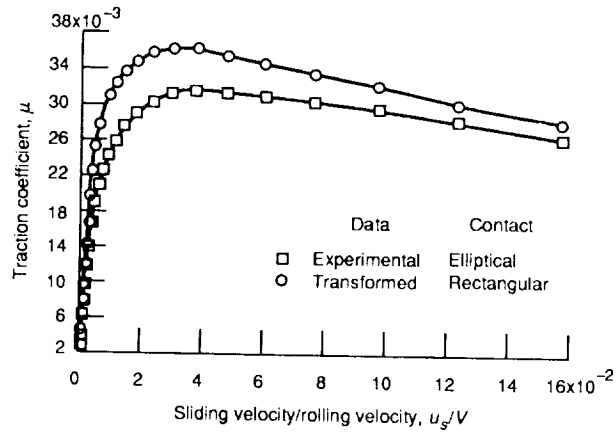

Figure 9.—Comparison of RP-1 experimental traction data for elliptical contact to analytically transformed traction data for equivalent rectangular contact. Contact pressure, 233 kpsi; velocity, 1200 in./sec; temperature, 104 °F.

the value of u_s^*, the sliding velocity at which μ^* occurs, tends to be lower for the line-contact data than for the elliptical data. The behavior of the transformed data is typical of that for other oils.

General trends of the RP-1 data.—Figure 10 shows a plot of μ/μ^* as a function of u_s/u_s^* for RP-1 for all conditions in the test matrix. Since the SHABERTH model of the traction curve is based on the assumption that μ/μ^* is a function of u_s/u_s^* only, it is desirable for the experimental data for μ/μ^* as a function of u_s/u_s^* to fall on one curve. In figure 10 the RP-1 data all follow the same general shape, though some scatter is present. The scatter is not deemed large enough to prohibit the use of the SHABERTH traction model.

Figure 11 shows the effect of maximum contact pressure on the values of μ^* and u_s^* for RP-1 at one condition of rolling velocity and fluid temperature. The behavior shown is typical over the range of conditions. The value of μ^* increases with increasing contact pressure, and the value of u_s^* decreases. In figure 12, the effect of rolling velocity on the values of μ^* and u_s^* for RP-1 is shown at one condition of contact pressure and temperature. Again, the behavior shown is typical over the range of conditions. The value of μ^* decreases with increasing rolling velocity, and the value of u_s^* increases.

Pressure-Viscosity Coefficient for RP-1

The SHABERTH code calculates a pressure-viscosity value as a function of temperature and lubricant ambient kinematic viscosity by using an expression developed by Fresco (ref. 6). This semiempirical model was developed by using data for fluids other than RP-1, and it accounts for different lubricant types only in the value of the viscosity. The coefficients used in the calculation are constant for all lubricant types. This model was not used in the analysis of the RP-1 data.

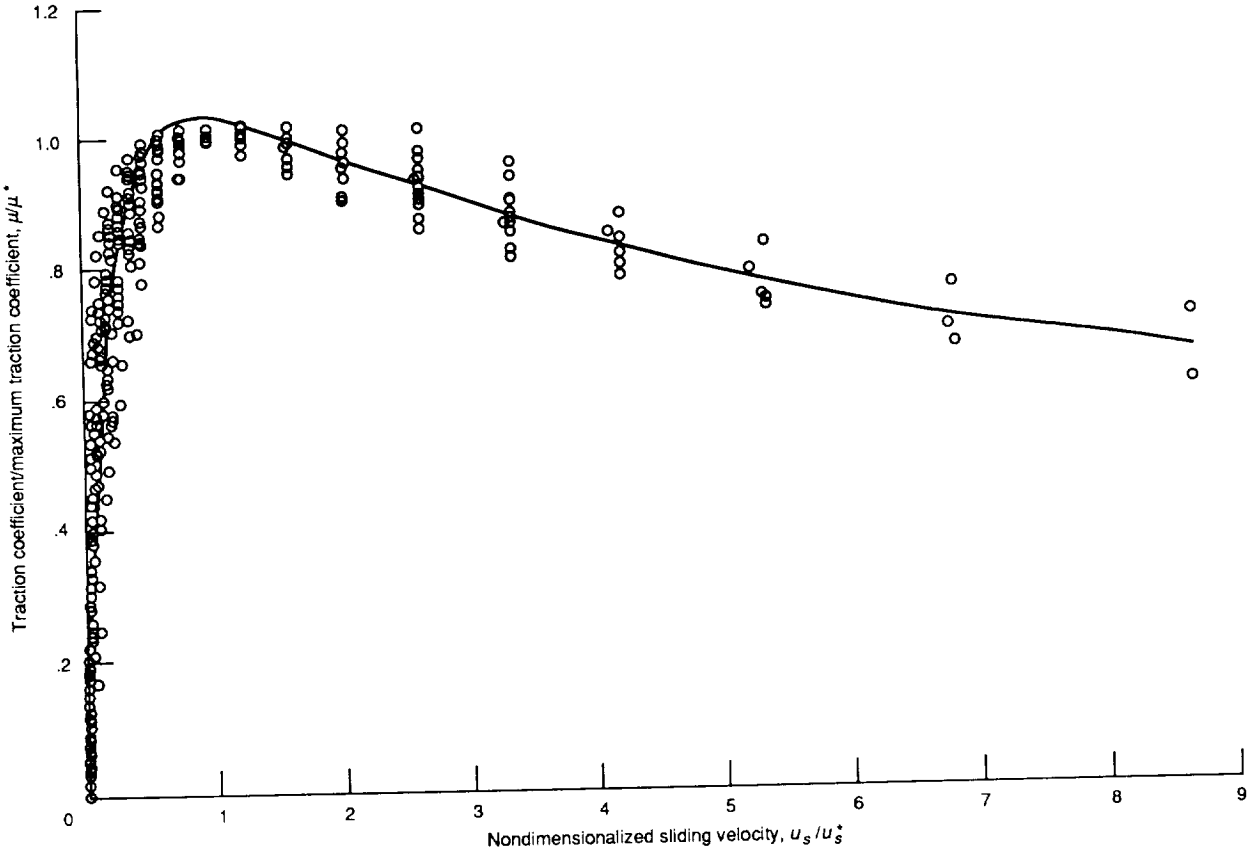

Figure 10.—RP-1 experimental data for μ/μ^* as a function of u_s/u_s^* for all test matrix conditions of maximum contact pressure, rolling velocity, and fluid temperature.

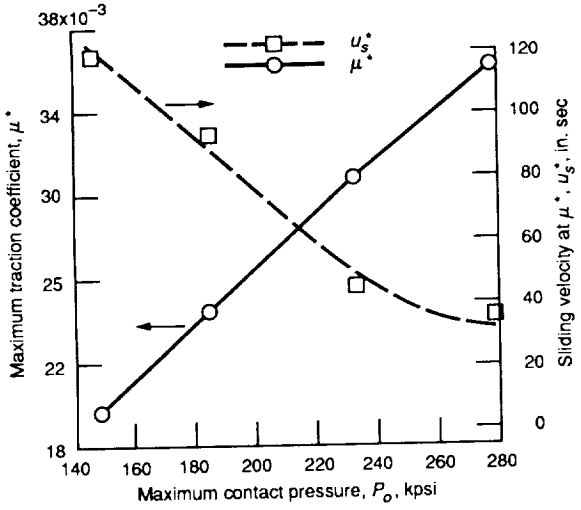

Figure 11.—Variation of RP-1 experimental maximum traction coefficient and associated sliding velocity with maximum contact pressure. Velocity, 2000 in./sec; temperature, 104 °F.

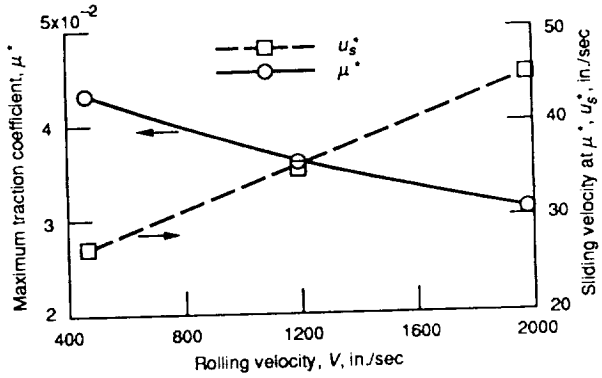

Figure 12.—Variation of RP-1 experimental maximum traction coefficient and associated sliding velocity with rolling velocity. Pressure, 233 kpsi; temperature, 104 °F.

As part of the effort to measure and analyze the traction data for RP-1, pressure-viscosity data generated by Bridgman for kerosene were obtained (ref. 12). The traction data specific to RP-1 were also used to check the validity of Bridgman's pressure-viscosity data for use with RP-1. By using the Barus pressure-viscosity relationship, that is,

$$\eta_P = \eta_\theta \exp\left[\left(\frac{B_I}{\theta + D_p}\right)\right] P \tag{28}$$

where

η_θ ambient absolute viscosity at inlet temperature, Pa-sec

θ inlet temperature, °C

D_p lubricant-dependent pressure solidification temperature, °C

B_I lubricant-dependent constant, °C/Pa

P pressure, Pa

and the reference 8 experimental data, the constants B_I and D_p were determined for RP-1 as $B_I = 544$ °C/Pa and $D_p = 25.6$ °C (ref. 8). This was the pressure-viscosity calculation used in fitting the RP-1 traction data to the SHABERTH traction model.

The pressure-viscosity coefficient α, which is used by SHABERTH, can be calculated from the Barus model by using

$$\alpha = \frac{B_I}{\theta + D_p} \tag{29}$$

and converting from units of Pascals^{-1} to square inches per pound.

Figure 13 shows the RP-1 pressure-viscosity coefficient as a function of temperature for both the Fresco and Barus models. The Fresco model predicts a nearly linear relationship between the pressure-viscosity coefficient and temperature, whereas the Barus model predicts a hyperbolic relationship. The difference between the two models' pressure-viscosity values was deemed significant enough to justify changing the SHABERTH code so that it would branch to equation (29) (with the appropriate values of B_I and D_p) instead of using the Fresco model when the lubricant is RP-1.

Fluid Traction Parameters

The final values of the SHABERTH fluid traction parameters obtained by fitting the RP-1 traction data to the previously discussed models are listed in appendix A. Also specified are other changes that need to be made to the SHABERTH code to run it with RP-1 as the lubricant choice.

Viscoelastic parameters.—The value of λ_0 was determined from equation (17) after a best-fit value of γ_3 was found. This value was obtained by varying γ_3 from its lowest to highest experimentally derived value, while comparing the predicted μ to the transformed experimental μ over all conditions, and choosing the γ_3 that gave the lowest

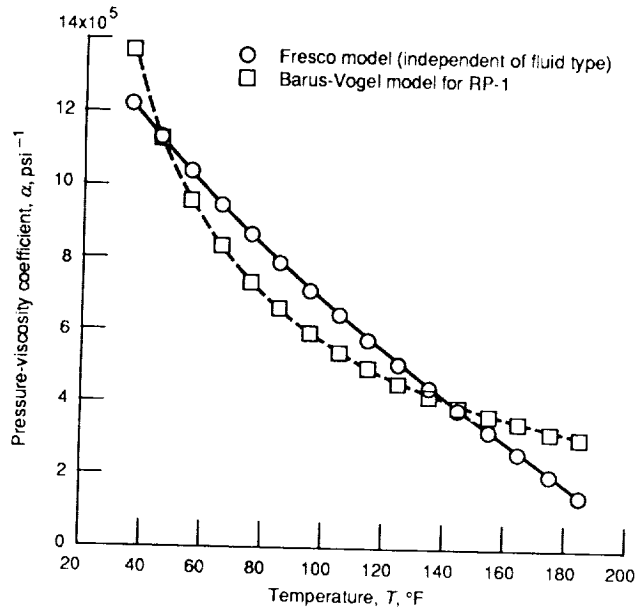

Figure 13.—Variation of pressure-viscosity coefficient for RP-1 with temperature—comparison of Fresco model (fluid-independent) and Barus-Vogel model.

average percent error over the pressure and temperature range. The resulting value was $\gamma_{3\,\text{final}} = -0.28$, which gives $\gamma_{0\,\text{final}} = 0.733$.

The function $f(P_o)$ was calculated from equations (10) and (14) by using $\lambda_0 = 0.733$ and $V_0 = 390$ in./sec. The relationship between $f(P_o)$ and P_o is shown in figure 14 at a particular rolling velocity and temperature; this behavior is typical at all conditions. No change in slope occurs in the plot of $\log[f(P_o)]$ with respect to $\log[P_o]$, thereby indicating that the expected decrease in the exponent A_i does not occur within the experimental range of maximum contact pressure. This is true at all conditions of speed and temperature in the matrix. However, based on the behavior of other fluids under high pressures (refs. 10 and 11), an assumption can be made that for RP-1, there is a P_1 at which the value of the exponent A_i decreases from A_1 to A_2. Since P_1 cannot be determined from the present experimental data, the value of A_1, which was obtained from experimental data, will be assumed to be valid up to a pressure 20 percent higher than the highest maximum contact pressure in the test matrix. This choice gives some weight to the experimentally derived data, while providing a safety valve against predicting unreasonably large values for viscosity. Therefore, $P_1 = 340\,000$ psi.

In order to model $f(P_o)$ as a function of P_o only, the data for $f(P_o)$ with respect to P_o for all conditions of rolling velocity and fluid temperature should fall on the same curve. Figure 15 shows the variation of $f(P_o)$ with P_o for all of the conditions and shows the best-fit line. Note that a considerable amount of scatter exists.

Figure 16 again shows the variation of $f(P_o)$ with P_o for all conditions, but the data sets taken at the two fluid

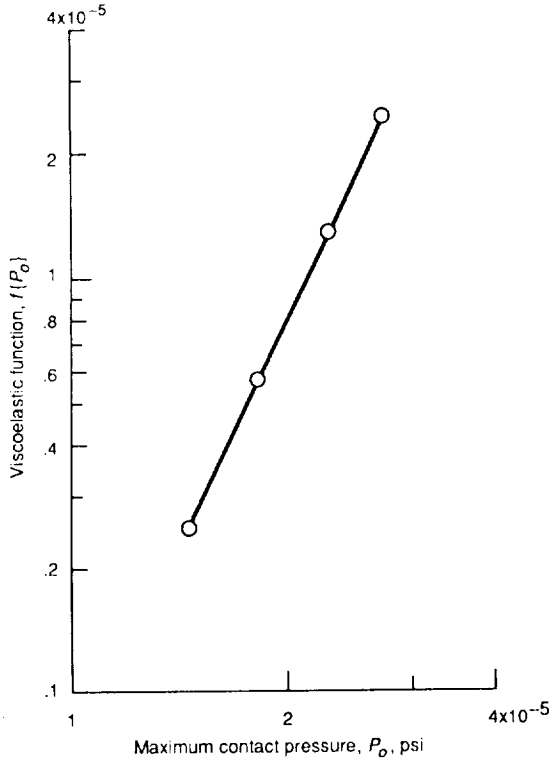

Figure 14.—Variation of viscoelastic function with maximum contact pressure for RP-1. Velocity, 1970 in./sec; temperature, 110 °F.

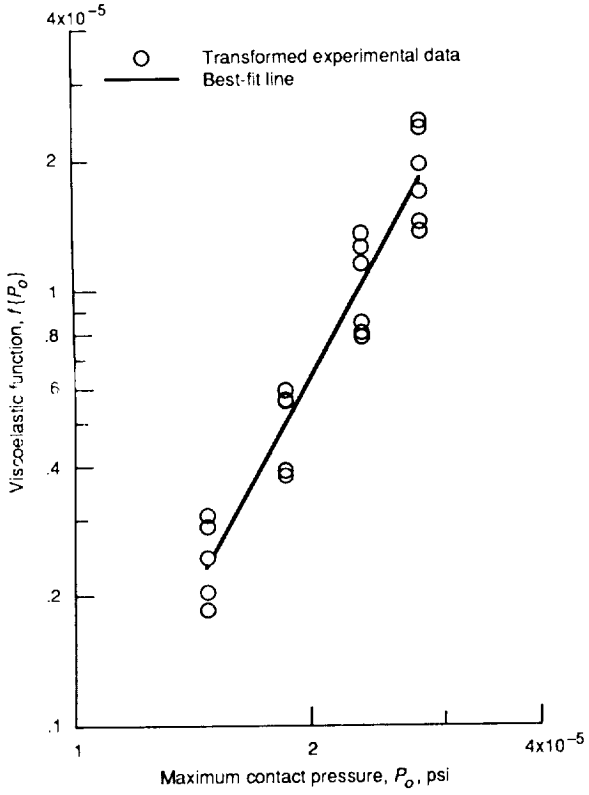

Figure 15.—Variation of viscoelastic function with maximum contact pressure for RP-1 at all test matrix conditions.

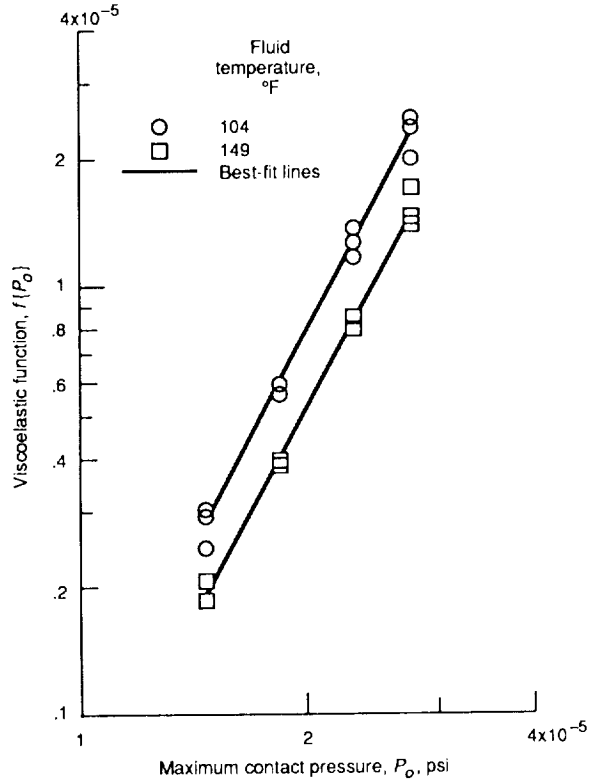

Figure 16.—Data and best-fit lines showing variation of viscoelastic function with maximum contact pressure for RP-1 at two temperatures.

temperatures are plotted separately and the best-fit line is drawn through each. From this figure, it is apparent that temperature has an effect on the relationship. The value of A_1 remained constant at both temperatures; only C_n is a function of temperature. Therefore, A_1 can be calculated without regard to the effect of temperature. The best-fit value obtained for A_1 was 3.23.

The value of A_2 cannot be determined directly from the experimental data since it occurs outside of the test matrix. The best alternative is to choose a value for A_2/A_1 based on the behavior of other fluids and determine A_2 from the value of A_1 for RP-1. The only fluid data in the SHABERTH reference material showing a decrease in A_i within the experimental test matrix are those for Shell Turbo 33, obtained by Johnson and Cameron (ref. 10). Their data give $(A_2/A_1)_{\text{Shell Turbo 33}} = 0.635$.

For the same reasons stated in the section Issues Concerning the SHABERTH Fluid Traction Model, A_2/A_1 for RP-1 was chosen as a lower value than that for Shell Turbo 33. For convenience, the value chosen was $(A_2/A_1)_{\text{RP-1}} = 0.5$, giving $A_2 = 1.6$.

An additional point can be made here concerning the RP-1 parameters. The particular value chosen for A_2 is not of critical importance to the traction prediction for RP-1. The range of pressures in which A_1 is valid should cover all cases in which the fluid traction plays a significant role. At higher contact pressures, the traction force prediction is governed

TABLE II.—VALUES OF C_1 AND C_2 FOR VARIOUS CASES

Equations used	Temperature-averaged values		Temperature-dependent values			
			At 104 °F		At 149 °F	
	C_1	C_2	C_1	C_2	C_1	C_2
(19) and (20)	113 450	24.65	126 456	21.40	99 262	28.19
(26) and (27)	629 519	136.40	700 536	118.01	552 045	156.46

predominantly by the dry asperity traction model. However, a value for A_2 should be coded in case it is required.

There is currently no mechanism in the SHABERTH program to handle a temperature-dependent f/P_o. Because there were only two conditions of temperature in the RP-1 experimental matrix, this study describes the error involved in ignoring the temperature dependency, but it does not develop a temperature-dependent algorithm.

Proportionality constants.—The temperature-dependent constant C_n in equation (18) is contained in the general proportionality constants C_1 and C_2, which must be found by fitting the transformed experimental RP-1 μ^* and u_s^* data to equations (19) and (20), once the viscoelastic parameters have been determined. Therefore, C_1 and C_2 reflect the temperature dependency encountered in the f/P_o data. The values chosen for these constants are the average of the best-fit values obtained at each temperature. The error resulting from the temperature-averaged values of C_1 and C_2 will be quantified in the section Results and Comparisons by comparing the traction predicted by using them to the traction predicted by using the values of C_1 and C_2 obtained at each temperature.

The values of C_1 and C_2 are also affected by the potential correction to equations (19) and (20), which led to equations (26) and (27). Therefore, in the Results and Comparisons section, the correction to the exponent of P_o will be shown to have a negligible effect on the resulting value of μ^*. Equations (19) and (20) are used in all subsequent calculations to determine values of C_1 and C_2. The values ultimately chosen for use in the SHABERTH code were the temperature-averaged values found by using the uncorrected equations (19) and (20); that is, $C_1 = 113\ 450$ and $C_2 = 24.65$.

Table II lists the values of C_1 and C_2 found for the various cases described above, that is, the temperature-averaged and temperature-dependent values needed for the uncorrected equations (19) and (20) and the corrected equations (26) and (27).

Traction curve shape parameters.—As stated previously, the traction curve predicted by SHABERTH follows a fixed mathematical function, increasing linearly at low sliding speeds and then asymptotically approaching the value of μ^*. Values of X_B and Y_B obtained from the nondimensionalized curve of μ/μ^* as a function of u_s/u_s^* are used to calculate μ as a function of u_s from equation (21), once μ^* and u_s^* are known. The values of X_B and Y_B that were found from the RP-1 data were 0.15 and 0.65 respectively.

Results and Comparisons

In this section the effect of the correction to the exponent of P_o in equations (19) and (20) will be shown to be negligible. The term "experimental data" will be used to mean the equivalent line-contact data that was transformed from the experimental elliptical data. Figure 17 shows a comparison of curves of μ as a function of u_s/V. These curves were generated by the SHABERTH model at test matrix conditions by using the corrected ((19) and (20)) and uncorrected ((26) and (27)) equations with the appropriate values of C_1 and C_2 for each. For reference, the experimental curve at the same conditions is also shown. For both SHABERTH curves, the effect of temperature on f/P_o has been neglected (i.e., C_1 and C_2 are temperature-averaged values). The value of the maximum traction coefficient of the corrected curve exceeds that of the uncorrected curve by 5 percent. Over the range of conditions, the maximum difference in the two predicted values of μ^* was 5 percent, with an average difference of 3 percent. The percentages for maximum and average differences in the values of u_s^* were comparable to those of μ^*.

In figure 18, which shows corrected and uncorrected curves at an extrapolated condition of pressure (330 kpsi) and rolling velocity (3937 in./sec), the curves differ by 6 percent.

As was stated previously, the values of the proportionality constants C_1 and C_2 that were hard-coded for the original lubricants would need to be recalculated by using the original traction data if equations (26) and (27) were to be substituted for equations (19) and (20). However, for a 1- to 5-percent difference in the value of μ^*, recalculation does not seem worth the effort.

Neglecting the temperature dependency of C_1 and C_2, though, has a greater effect on the results. Figures 19 and 20 compare experimental traction curves at various conditions, not only to those predicted by using temperature-averaged values of C_1 and C_2 but also to those predicted by using temperature-dependent values of C_1 and C_2.

The curves in figure 19 are all at the lower temperature condition (104 °F). In all cases the temperature-dependent curves predict the value of μ^* quite well. The errors between the experimental values of μ^* and those predicted by using temperature-dependent C_1 and C_2 are, respectively, 2.6, 0.6, 0.3, and 1.2 percent for the four cases shown. Over the range

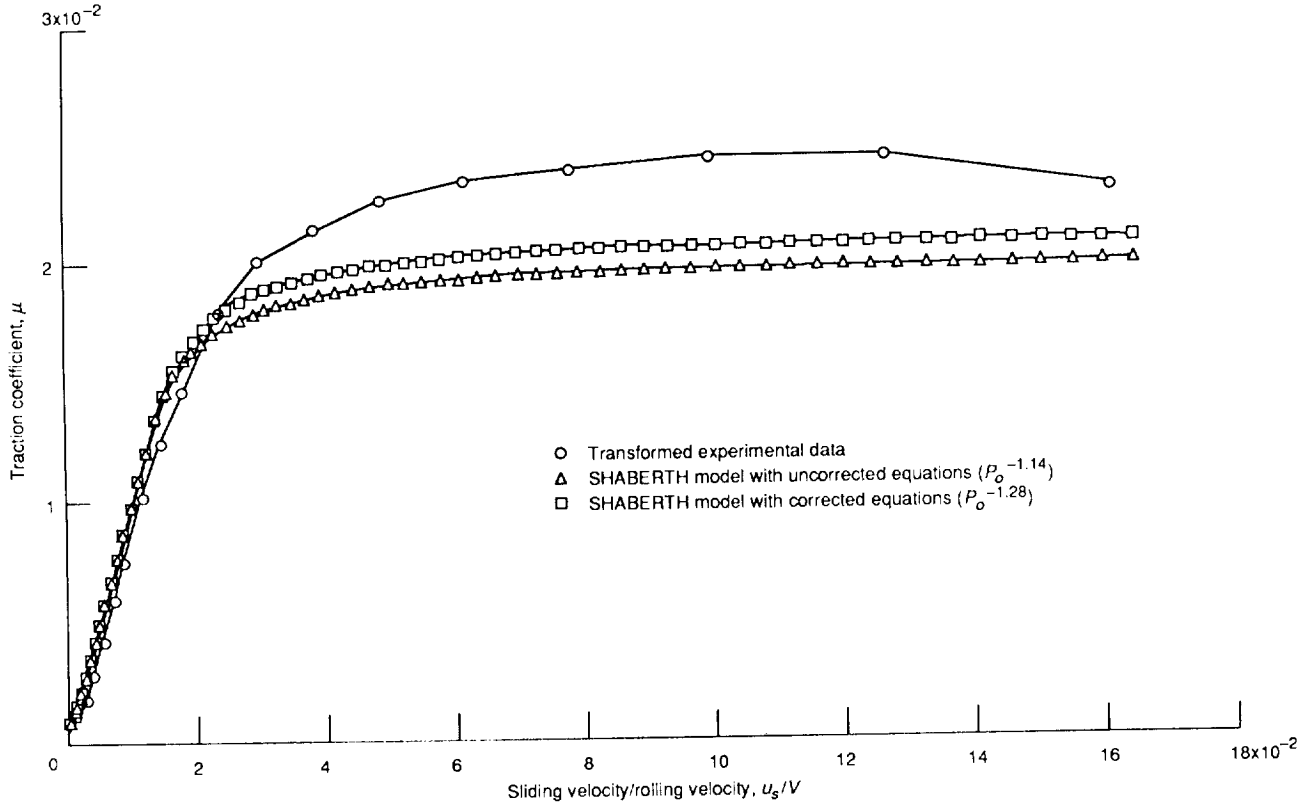

Figure 17.—Comparison of SHABERTH predictions for RP-1 using uncorrected and corrected traction equations. Contact pressure, 147 kpsi; velocity, 1181 m/sec; temperature, 95 °F. (Transformed experimental data shown for reference.)

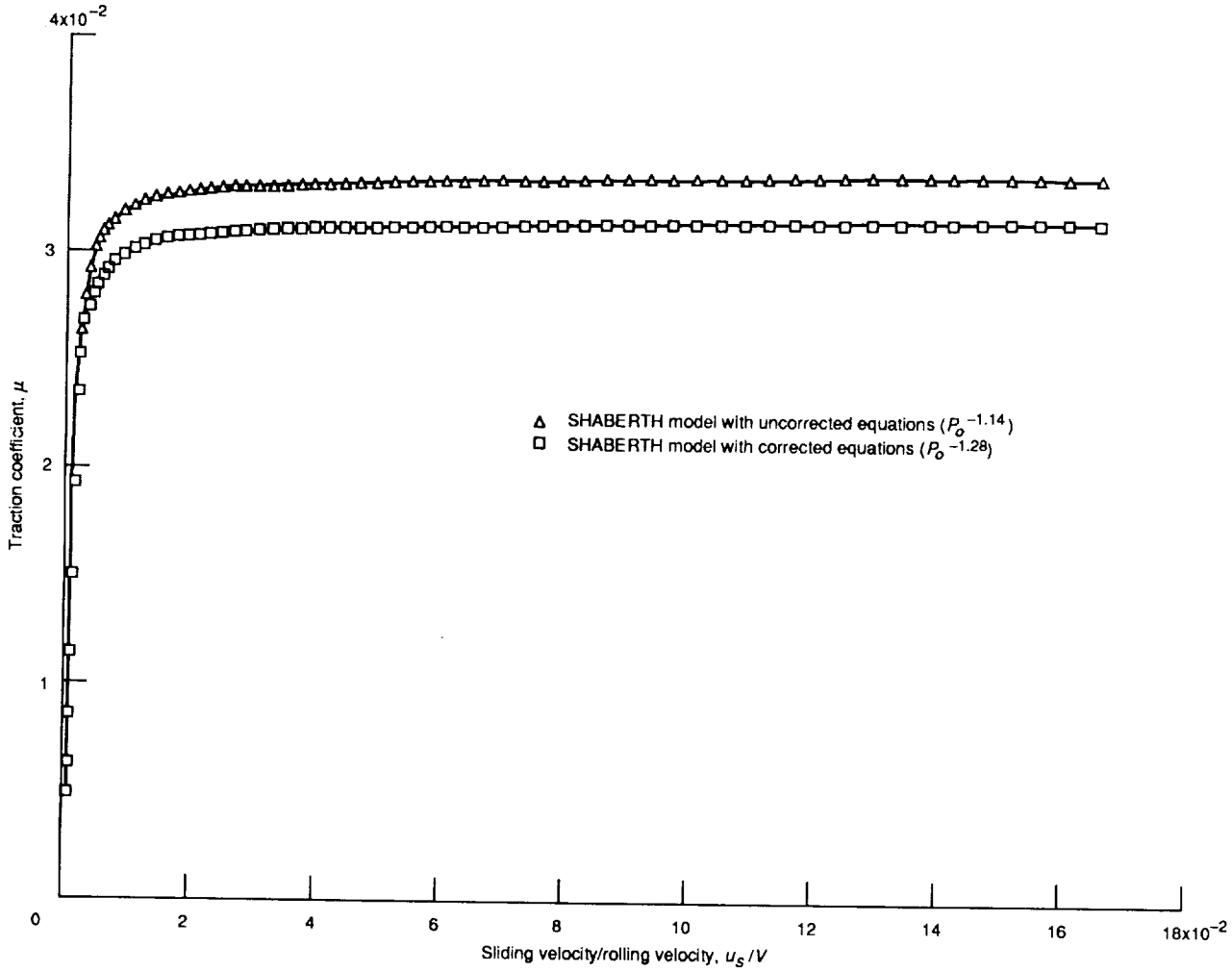

Figure 18.—Comparison of SHABERTH predictions for RP-1 using uncorrected and corrected traction equations at extrapolated conditions. Contact pressure, 330 kpsi; velocity, 3937 in./sec; temperature, 104 °F.

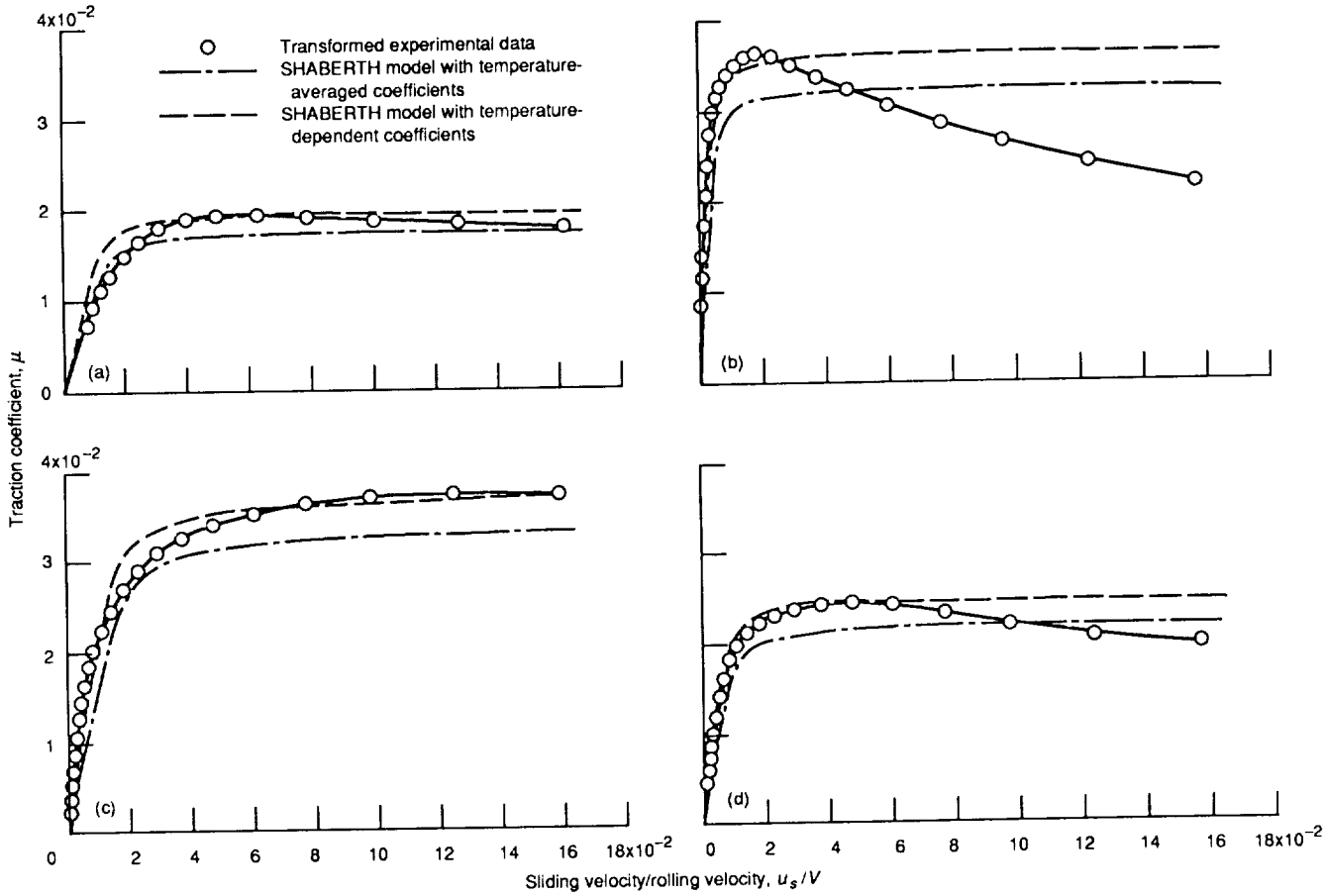

(a) Low maximum contact pressure: P_o, 147 kpsi (velocity, 1953 in./sec).
(b) High maximum contact pressure: P_o, 279 kpsi (velocity, 1969 in./sec).
(c) Low rolling velocity: V, 445 in./sec (P_o, 185 kpsi).
(d) High rolling velocity: V, 1969 in./sec (P_o, 185 kpsi).

Figure 19.—Traction coefficient of RP-1 as a function of slide-to-roll ratio at 104 °F—comparison of curves from transformed experimental data with those from SHABERTH predictions using temperature-averaged and temperature-dependent coefficients.

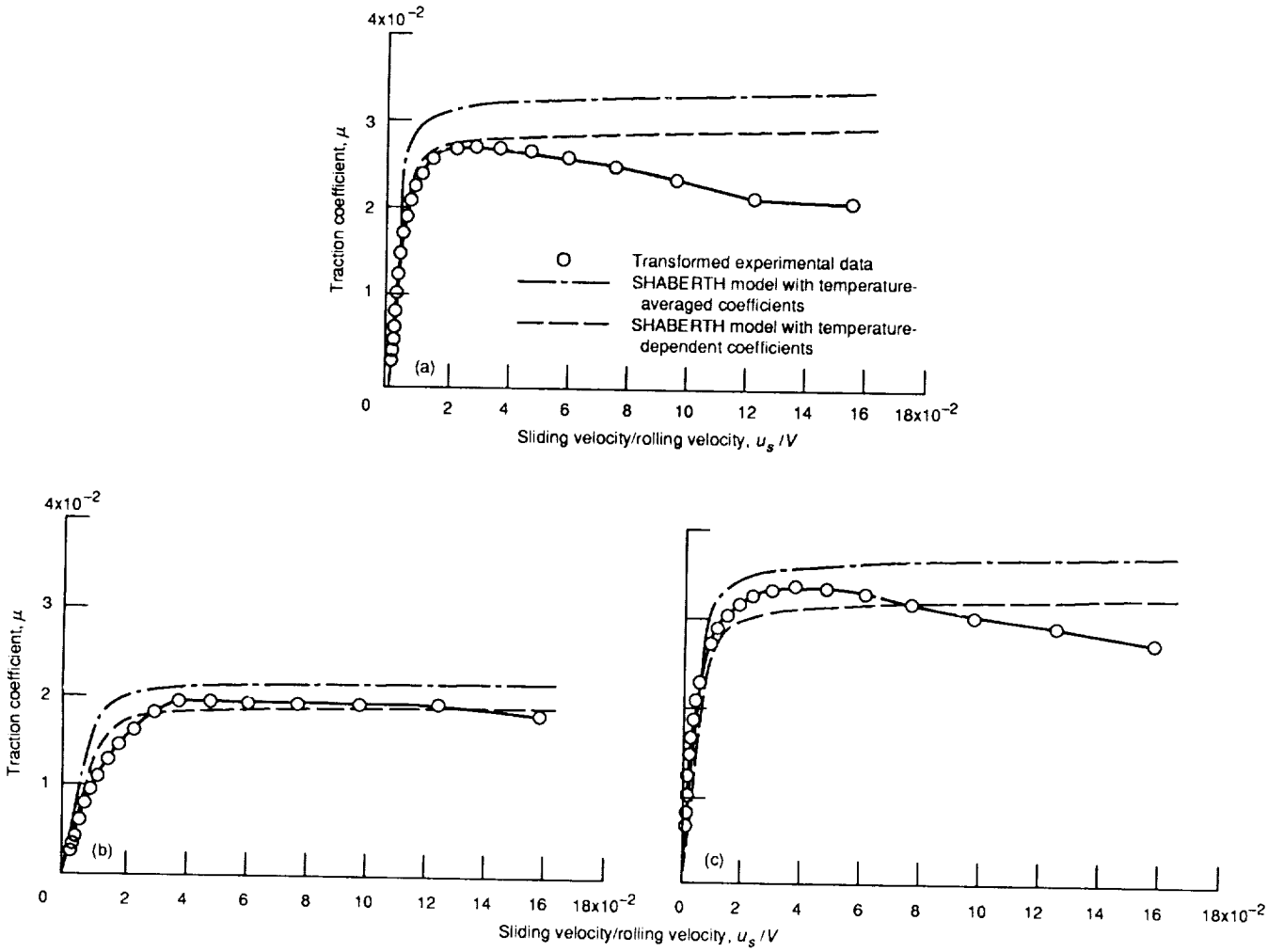

(a) High maximum contact pressure, high rolling velocity: P_o, 279 kpsi; V, 1953 in./sec.
(b) Low maximum contact pressure: P_o, 185 kpsi (velocity, 1969 in./sec).
(c) Low rolling velocity: V, 1200 in./sec (P_o, 279 kpsi).

Figure 20.—Traction coefficient of RP-1 as a function of slide-to-roll ratio at 149 °F—comparison of curves from transformed experimental data with those from SHABERTH predictions using temperature-averaged and temperature-dependent coefficients.

of conditions at the lower temperature, the average error was 3.4 percent and the highest error, 8.2 percent.

Since the value of μ^* decreases with increases in temperature, the use of the temperature-averaged values of C_1 and C_2 underpredicts the experimental values at the lower temperature. In the cases shown, the values of μ^* from using temperature-averaged C_1 and C_2 differ from the experimental ones by 8.2, 9.9, 10.0, and 9.3 percent respectively. The average error in μ^* over the range of conditions at the lower temperature was 10.3 percent, and the highest error was 17.9 percent.

Figure 19 also shows that the accuracy with which the shape of the traction curve is predicted varies with contact pressure and rolling velocity. As a result of SHABERTH's asymptotically increasing model of the traction curve, any thermal dissipation effects, that is, decreasing traction at high u_s/V, are completely neglected. Of greater importance, however, is the prediction of the low u_s/V region, since ball sliding in a bearing occurs predominantly at low u_s/V.

Parts (a) and (b) of figure 19 show curves at conditions of different maximum contact pressures, but of the same rolling velocity. At low contact pressure (fig. 19(a)) the effect of thermal dissipation is small, and the predicted temperature-dependent curve agrees well with the experimental one at high u_s/V. At low u_s/V, however, the SHABERTH curve both overpredicts the initial slope and remains linear up to a higher u_s/V than does the experimental curve. At high contact pressure (fig. 19(b)) the thermal effect at high u_s/V is much more pronounced and, thus, not well predicted by SHABERTH. However, the initial portion of the curve is better predicted at the higher contact pressure, almost exactly matching the shape of the experimental curve up to 0.015 u_s/V.

Parts (c) and (d) of figure 19 show the effect of rolling velocity on the shape of the curve at the same contact pressure. At low rolling velocity (fig. 19(c)) the high u_s/V region is well predicted because of the absence of significant thermal effects, but the initial slope is underpredicted. Also, the predicted curve remains linear up to a higher u_s/V than does the experimental curve. The high rolling velocity curves in figure 17(d) show that the thermal effect increases with rolling velocity, thereby causing greater discrepancies at high u_s/V. The initial portion of the curve is, however, very well predicted, accurately matching the shape of the curve up to 0.06 u_s/V.

The results at the higher temperature (149 °F) were very similar (see fig. 20). Again, the values of μ^* obtained by using temperature-dependent C_1 and C_2 show good agreement with the experimental ones. For the conditions shown in figure 20 parts (a) to (c), the temperature-dependent prediction of μ^* differs from the experimental prediction by 5.9, 1.5, and 3.9 percent respectively. The average error over the range of conditions at this temperature was 4.1 percent, and the highest error, 9.8 percent. The values of μ^* determined by using temperature-averaged values of C_1 and C_2 overpredicted the experimental μ^* by 21.1, 12.2, and 9.9 percent in figure 20 parts (a) to (c), respectively. The average error was 14.4 percent and the highest, 25.3 percent.

The same trends in ability to predict the shape of the traction curve are seen at the higher temperature as at the lower. Figure 20(a) shows curves at a condition of high contact pressure and high rolling velocity. The initial portion of the curve is very well predicted up to 0.03 u_s/V, whereas the high u_s/V region is not well predicted because of thermal dissipation effects. At a lower contact pressure and the same rolling velocity (fig 19(b)), the high u_s/V region is well predicted, but the predicted curve at low u_s/V remains linear up to a higher u_s/V ratio than does the experimental one. Figure 20(c) shows curves at the same contact pressure as in figure 20(a) but at a lower rolling velocity. As in the low-temperature case, the initial slope of the curve is underpredicted. There is still a significant thermal effect in this experimental curve because of the high contact pressure.

In general, the error from using temperature-averaged values of C_1 and C_2 runs approximately 10 percent higher than that from using the discrete, temperature-dependent values. The traction model for RP-1 does very well (1) at predicting the shape of the low u_s/V region of the traction curve at conditions of high maximum contact pressure and high rolling velocity and (2) at predicting the shape of the high u_s/V region at conditions in which thermal dissipation does not play a significant role (i.e., low maximum contact pressures and low rolling velocities). At conditions of low contact pressure or low rolling velocity, the initial slope of the traction curve is not well predicted, and the predicted curves remain linear up to higher u_s/V values than do the experimental curves.

Concluding Remarks

An effort is underway both to provide data on and to develop a bearing design methodology for Rocket Propellant 1 (RP-1), a hydrocarbon fuel, for possible use in future engine programs. Integral to this effort is the modification of the rolling-element bearing analytic code SHABERTH to incorporate RP-1 as a bearing lubricant. Modification of the code requires that certain specific property data be hard-coded. Of the required data, the only information not previously known for RP-1 were the characteristics of traction force as a function of shear rate; these characteristics must be determined experimentally. The traction data were obtained and fit into the traction model of SHABERTH, thereby providing a set of parameters that were hard-coded.

A slight error was detected in the traction equations that are in the SHABERTH program. However, lack of traction data on the original lubricants prevented immediate correction of the error. The error was found to make an insignificant difference in predicting traction for RP-1. A particular traction coefficient for RP-1 was found to be temperature-dependent; this is not accounted for by the model. Prediction of the maximum traction coefficient by using temperature-averaged coefficients erred by an average of 12 percent, whereas prediction by using the discrete coefficients at the two temperature conditions erred by an average of 4 percent. Currently, the temperature-averaged coefficients are being used. Future work may include developing and adding a temperature-dependent coefficient into the model. The model of the pressure-viscosity coefficient as a function of temperature was tailored to RP-1 by using RP-1 pressure-viscosity data.

A potential project is the investigation of more recent traction models, with the possible replacement of the present traction model in the SHABERTH code in mind. Much work has been done in the area of traction modeling since the development of the SHABERTH code. It is now possible to reduce the traction data to a few fundamental parameters from which the entire traction curve can be predicted with good accuracy, including the high slide-to-roll region where thermal dissipation can become a significant factor.

One such model, which has shown very good agreement with experimental data on a wide variety of lubricants and which would be a good candidate to replace SHABERTH, is the Johnson-Tevaarwerk model. In addition to its ability to accurately predict fluid traction due to ball sliding, the Johnson-Tevaarwerk model has demonstrated the capability to take into account spin and asperity contact as well. Further experimental work on RP-1, as well as work on the SHABERTH code, would be needed for the spin and asperity options.

Lewis Research Center
National Aeronautics and Space Administration
Cleveland, Ohio, April 17, 1990

Appendix A
Changes to the SHABERTH Code

This appendix describes the changes which must be made to the SHABERTH code in order to incorporate RP-1 as a lubricant choice. It includes the modified portions of the SHABERTH code.

A fifth lubricant choice, Freon E-1, was added to the code in 1986. Some versions of the code may not have this addition. The code listed herein has all of the necessary information for adding both the Freon E-1 and the RP-1 choices.

VISCO2

In the subroutine VISCO2, lines 2, 3, 4, and 11 must be added. The variable NCODE must be added to the input list in both the subroutine statement and the call statements. The following information is contained in these additions:

BB = 544. (constant B_I in Barus pressure-viscosity relationship, 1/GPa)

DP = 25.6 (pressure solidification temperature D_p in Barus pressure-viscosity relationship, °C)

VISCO2

```
1       SUBROUTINE VISCO2 ( NCODE,A,B,TEMP,RHO60, G, VISCP, ALO, RHO )

2       BB = 544.
3       DP = 25.6
4       TT = (TEMP - 32.)*(5./9.)

5       C = 10.**A
6       EXP = C / ( TEMP + 459.7 )**B
7       VISCS = 10.**EXP - .6
8       RHO = RHO60 - G * ( TEMP - 60. )
9       VISCP = RHO * VISCS

10      CALL ALPHAO ( B*.2, VISCS, TEMP+459.7, ALO )
11      IF (NCODE.EQ.6) ALO = (BB/(TT+DP))*6.894E-06

12      RETURN
13      END
```

EHDSKF

In the subroutine EHDSKF, the following variable values must be added at the end of each appropriate data list in the DATA statement (lines 3 to 8). Also, in line 9, 'N .LT. 6' must be changed to 'N .LT. 7'.

C1 = 113450. (C_1)
C2 = 24.65 (C_2)
C3 = 0.0329 ($0.48 - 0.61\lambda_0$)
C4 = 0.203 ($0.4\lambda_0 - 0.09$)
A1 = 3.23 (A_1)
A2 = 1.6 (A_2)
P1 = 3.4E5 (P_1)
SLB = 0.15 (X_B)
FBK = 0.65 (Y_B)

EHDSKF

```
1       SUBROUTINE EHDSKF( ET, H, V, PO, US, N, UM )
2       DIMENSION C1(6),C2(6),C3(6),C4(6),A1(6),A2(6),P1(6),SLB(6),FBK(6)
```

```
3      DATA C1/4734.5,46293.,68910.,27350.,28000.,113450./, C2/304.848,
4     1102.58,17.31,124.4226,125.012,24.65/, C3/0.297,-0.0934,0.053,
5     2-0.0873,-0.0881,.0329/,C4/0.03,0.286,0.19,0.282,0.284,0.203/,A1/
6     33.42,4.08,3.29,6.88,6.80,3.23/, A2/2.14,1.48,1.5,3.44,3.40,1.6/,
7     4P1/1.5E5,1.7E5,1.7E5,2.2E5,2.0E5,3.4E5/, SLB/0.1,0.25,0.15,0.25,
8     50.25,0.15/, FBK/0.65,0.68,0.65,0.68,0.68,0.65/

9      IF( N .GT. 0 .AND. N .LT. 7 )     GO TO 10

10     KT = 6
11     WRITE(KT,100)
12  100 FORMAT('0',119('*'),/'0 AN IMPROPER LUBRICANT TYPE CODE HAS BEEN
13    $PASSED TO EHDSKF.  EXECUTION TERMINATES'/'0',119('*') )
14     STOP

15   10 CONTINUE
16     UM = 1.E-8
17     IF ( PO .LT. 1000. ) RETURN
18     IF ( PO .LT. P1(N) ) X1 = (PO/P1(N)) ** A1(N)
19     IF( PO .GT. P1(N) ) X1 = (PO/P1(N) ) ** A2(N)
20     UMS = C1(N) / PO**1.14 * X1**0.61 * ET**0.59 * V**C3(N) / H**0.45
21     USS = C2(N)/PO**0.14/X1**0.4/ET**1.1 * V**C4(N) * H**0.55
22     FBREAK = FBK(N)
23     SVB = SLB(N)
24     SV = US/USS
25     UM = UMS * FRICTN(FBREAK, SVB, SV )
26     RETURN
27     END
```

LUPROP

In the subroutine LUPROP. Text must be added to the DATA list in lines 8 and 9. In line 15, ',600' must be added to the GOTO statement. Lines 82 to 96 must be added. These lines contain the following information:

VIS1 = 1.571	(kinematic viscosity at 100 °F, cSt)
VIS2 = 0.7542	(kinematic viscosity at 210 °F, cSt)
A = 13.98464	(constant in Walther's equation)
B = 5.26787	(constant in Walther's equation)
RHO60 = 0.8065	(fluid density at 60 °F, g/cm^3)
G = 7.2E-04	(fluid thermal expansion coefficient, 1/°C)
COND = 0.13806	(fluid thermal conductivity, W/m °C)
BETA = 0.007278	(auxiliary temperature-viscosity coefficient, 1/°R)
AKN = 20.	(EHD high-contact stress factor—not used with the SKF fluid traction model)
FRIC = 0.070	(Allen friction coefficient—not used with the SKF fluid traction model)

LUPROP

```
1      SUBROUTINE LUPROP ( NCODE, KK, A, B, BETA, RHO60, G, COND, VIS1,
2     $  VIS2, XLUBE, IMET )

3      DIMENSION AL(9,6), XLUBE(9,6)

4      COMMON /FLMDAT/ EMOD(2), AKN, FRIC
```

```
      DATA AL /'  ','SH','EL','L ','TU','RB','O ','33','  ','  ',' M',
     1  'IL','-L','-7','80','8G','  ','  ','PL','YP','HN','L ','ET',
     2  'H ','MC','S2','93','  ',' M','IL','-L','-2','36','99','  ',
     3  '  ','  ','SP','EC','IA','L ','E1','  ','  ','  ','RO','CK',
     4  'ET',' P','RO','PE','LL','NT',' 1'/

... FILL XLUBE WITH THE APPROPRIATE ALPHMERIC LUBRICANT TYPE DATA.
        DO 10 I = 1,9
 10     XLUBE(I,KK) = AL(I,NCODE)
      KT = 6

... DETERMINE THE LUBRICANT TYPE FROM NCODE

      GO TO ( 100, 200, 300, 400, 500, 600 ), NCODE

100 CONTINUE
... THE LUBRICANT IS SHELL TURBO 33
      VIS1 = 64.
      VIS2 = 8.
      A = 10.34871
      B = 3.672531
      RHO60 = 0.879975
      G = 6.336E-4
      COND = 0.11614
      BETA = 0.01932
      AKN = 18.2
      FRIC = .075
      GO TO 999

200 CONTINUE
... THE LUBRICANT IS A MIL-L 7808G
      VIS1 = 12.76
      VIS2 = 3.2
      A = 10.214494
      B = 3.698398
      RHO60 = .9526
      G = 7.092E-4
      COND = 0.15218
      BETA = 0.013168
      AKN = 18.2
      FRIC = .045
      GO TO 999

300 CONTINUE
... THE LUBRICANT IS POLY PHENYL ETHER MCS 293
      VIS1 = 25.4
      VIS2 = 4.13

      A = 11.451954
      B = 4.112963
      RHO60 = 1.2006
      G = 7.47E-4
      COND = 0.11924
      BETA = 0.016798
      AKN = 24.9
```

```
      FRIC = .070
      GO TO 999

  400 CONTINUE
C     THE LUBRICANT IS A MIL-L-23699
      VIS1 = 28.
      VIS2 = 5.1
      A = 10.207208
      B = 3.655059
      RHO60 = 1.0102
      G = 7.452E-4
      COND = 0.15218
      BETA = 0.016089
      AKN = 18.2
      FRIC = .070
      GO TO 999

C     LUBRICANT ADDED FOR CRYOGENIC USE
C     E.S.ARMSTRONG, LEWIS RESEARCH CENTER, 4-10-86

  500 CONTINUE
C ....THE LUBICANT IS SPECIAL E1
      VIS1 = .4370
      VIS2 = .4106
      A = 17.2097
      B = 6.9177
      RHO60 = 1.564
      G = .002826
      COND = .06921
      BETA = .0180
      AKN = 20.
      FRIC = .070
      GOTO 999

C     LUBRICANT ADDED - LOW VISCOSITY FUEL
C     C. M. WOODS , LEWIS RESEARCH CENTER , 10/28/89

  600 CONTINUE
C .....THE LUBRICANT IS RP-1
      VIS1 = 1.571
      VIS2 = .7542
      A = 13.98464
      B = 5.26787
      RHO60 = 0.8065
      G = 7.2E-04
      COND = 0.13806

      BETA = 0.007278
      AKN = 20.
      FRIC = .070

  999 CONTINUE

      CONVERT TO ENGLISH INITS IF REQUIRED.
```

```
      IF( IMET .EQ. 1 )      GO TO 1000
      RHO60 = RHO60 * 0.036127
      G = G * 0.5555555
      VIS1 = VIS1 * 1.55E-3
      VIS2 = VIS2 * 1.55E-3
      COND = COND * 0.5777

1000  CONTINUE
      RETURN
      END
```

Appendix B
Symbols

A,B	constants in Walther's equation
A_i	generic expression for A_1 and A_2
A_1,A_2	parameters in the viscoelastic relationship
a	semimajor length of Hertzian contact ellipse, in.
a_1,a_2,a_3,c_1	exponents of the nondimensional traction equation
B_I	lubricant-dependent constant in Barus model, °C/Pa
b	semiminor width of Hertzian contact ellipse, in.
b_1,b_2	coefficients in geometric fit
b_3,b_4	coefficients in exponential fit
C_F,D_F,E_F	constants in the Fresco model
C_m	general constant of proportionality
C_n	constant in the viscoelastic relationship
C_q	constant in the film thickness relationship
C_1,C_2	constants of proportionality in traction equations
C_3,C_4	constants in traction equation
c_f	specific heat of fluid, Btu/°F-in.^{3}
D_p	pressure solidification temperature in Barus model, °C
d_0,d_1,d_2,d_3,d_4	coefficients in polynomial fit
E'	effective elastic modulus, lb/in.^{2}
G	fluid coefficient of thermal expansion, 1/°C
h	minimum film thickness, in.
K_f,K_f'	conductivity of fluid film, ft-lb/ft °F-sec; W/m °C, respectively
n_1	constant in film thickness relationship
P,P'	pressure, lb/in.^{2}; Pa, respectively
P_o	maximum Hertzian contact pressure, lb/in.^{2}
$f\{P_o\}$	function of P_o in viscoelastic relationship
P_1	parameter in the viscoelastic relationship, lb/in.^{2}
R_x	curvature sum in x-direction (rolling direction), in.
T	fluid temperature, °F
T_R	experimental traction force, lb
$\bar{T}_R$	average experimental traction force per unit length, lb/in.
$\bar{U}$	speed viscosity product
U_1,U_2	rolling velocity of disk 1 and disk 2, respectively, in./sec
u_s	sliding velocity, in./sec
u_s^*	sliding velocity at which μ^* occurs, in./sec
u_s/u_s^*	nondimensionalized sliding velocity
V	rolling velocity (entrainment velocity), in./sec
V_0	constant in the viscoelastic relationship, in./sec
X_B,Y_B	shape parameters for the predicted traction curve
x	coordinate in contact plane in direction of rolling, in.
x^*	coordinate of nondimensional curve for u_s/u_s^*
y	coordinate in contact plane normal to rolling, in.
y^*	coordinate of nondimensional curve for μ/μ^*
z	coordinate normal to contact plane, in.
α	pressure-viscosity coefficient, in.^{2}/lb
β	temperature-viscosity coefficient, 1/°R
β'	secondary pressure-viscosity coefficient, in.^{2}/lb
γ_3	exponent in the relationship of μ^* as a function of V
η_0,η_0'	ambient absolute viscosity at inlet temperature, lb-sec/in.^{2}; cP, respectively
$\eta_e,\eta\{p\}$	effective absolute viscosity in contact, lb-sec/in.^{2}; Pa-sec, respectively
$\eta\{\theta\}$	ambient absolute viscosity at inlet temperature, Pa-sec
θ	fluid inlet temperature, °C
λ_0	parameter in the viscoelastic relationship
μ	traction coefficient (tractive force/normal load)
μ'	nondimensionalized traction coefficient term
μ^*	maximum traction coefficient
$(\mu')^*$	maximum nondimensionalized traction coefficient term
ν	ambient kinematic viscosity at inlet temperature, cSt
ρ,ρ_f	fluid density, g/cm^3; lb/in.^{3}, respectively
σ	composite surface roughness, in.
τ_x	fluid shear stress in rolling direction, lb/in.^{2}
$(\psi_0^{1/2})$	nondimensionalized sliding velocity term
$(\psi_0^{1/2})^*$	nondimensionalized sliding velocity term at $(\mu')^*$

References

1. Butner, M.F., and Keller, R.B.: Liquid Rocket Engine Turbopump Bearings. NASA SP-8048, 1971.
2. Butner, M.F.: Propellant Lubricant Properties Investigation. DTIC Report WADD TR 61-77, 1961.
3. Reber, L.D.: Titan Liquid Engine Propulsion—Past, Present, and Future. AIAA Paper 86-1631, 1986.
4. Hadden, G.B., et al.: Research Report—User's Manual for Computer Program AT81Y003 SHABERTH. (SKF-A T81DO40, SKF Technology Services; NASA Contract NAS3-22690) NASA CR-165365, 1981.
5. McCool, J.I., et al.: Influence of Elastohydrodynamic Lubrication on the Life and Operation of Turbine Engine Ball Bearings. Bearing Design Manual. Air Force Contract No. F33615-72-C-1467, SKF Report AL73P014, 1973.
6. Crecelius, W.J.; and Pirvics, J.: Computer Program Operation Manual on "SHABERTH": A Computer Program for the Analysis of the Steady State and Transient Thermal Performance of Shaft-Bearing Systems. Air Force Report AFAPL-TR-76-90, 1976.
7. Piper, L.B., ed.: Liquid Propellant Manual CPIA/M4. Chemical Propulsion Information Agency, Johns Hopkins University, 1982.
8. Tevaarwerk, J.L.: The Measurement, Modeling, and Prediction of Traction for Rocket Propellant 1. NASA CR-185186, 1990.
9. Tevaarwerk, J.L.: Thermal Contact Performance Evaluation Under Fully Flooded and Starved Conditions. NASA CR-168173, 1985.
10. Johnson, K.L.; and Cameron, R.: Shear Behavior of EHD Oil Film at High Rolling Contact Pressure. Proceedings of the Institution of Mechanical Engineers, Tribology Group, Vol. 182, Westminister, London WE1, 1968, pp. 307-330.
11. Allen C.W.; Townsend, D.P.; and Zaretsky, E.V.: Elastohydrodynamic Lubrication of a Spinning Ball in a Nonconforming Groove. J. Lubr. Technol., vol. 92, no. 1, Jan. 1970, pp. 89-96.
12. Bridgman, P.W.: The Physics of High Pressure. Dover Publications, New York, 1970.

NASA
National Aeronautics and Space Administration

Report Documentation Page

1. Report No.	2. Government Accession No.	3. Recipient's Catalog No.
NASA TP-3017		

4. Title and Subtitle	5. Report Date
Modification of the SHABERTH Bearing Code To Incorporate RP–1 and a Discussion of the Traction Model	September 1990
	6. Performing Organization Code

7. Author(s)	8. Performing Organization Report No.
Claudia M. Woods	E-5407
	10. Work Unit No.
	590-21-11

9. Performing Organization Name and Address	11. Contract or Grant No.
National Aeronautics and Space Administration Lewis Research Center Cleveland, Ohio 44135-3191	
	13. Type of Report and Period Covered
	Technical Paper

12. Sponsoring Agency Name and Address	14. Sponsoring Agency Code
National Aeronautics and Space Administration Washington, D.C. 20546-0001	

15. Supplementary Notes

16. Abstract

Recently developed traction data for Rocket Propellant 1 (RP-1), a hydrocarbon fuel of the kerosene family, was used to develop the parameters needed by the bearing code SHABERTH in order to include RP-1 as a lubricant choice. The procedure for inputting data for a new lubricant choice is reviewed, and the theoretical fluid traction model is discussed. Comparisons are made between experimental traction data and those predicted by SHABERTH for RP-1. All data needed to modify SHABERTH for use with RP-1 as a lubricant are specified.

17. Key Words (Suggested by Author(s))	18. Distribution Statement
SHABERTH; Traction; RP-1; Bearings; Computer code	Unclassified – Unlimited Subject Category 37

19. Security Classif. (of this report)	20. Security Classif. (of this page)	21. No. of pages	22. Price*
Unclassified	Unclassified	30	A03

*For sale by the National Technical Information Service, Springfield, Virginia 22161

National Aeronautics and
Space Administration
Code NTT-4

Washington, D.C.
20546-0001